High-energy gamma-rays from magnetically arrested disks in nearby radio galaxies

Riku Kuze (Tohoku Univ.)
Dr. Shigeo S. Kimura (Tohoku Univ.)
Dr. Kenji Toma (Tohoku Univ.)

Reference: **Riku Kuze**, Shigeo S. Kimura, and Kenji Toma., arXiv 2205.09565
ApJ in press.

TeVPA 2022, Kingston, Queen's University, 8-12 Aug 2022

Radio Galaxies

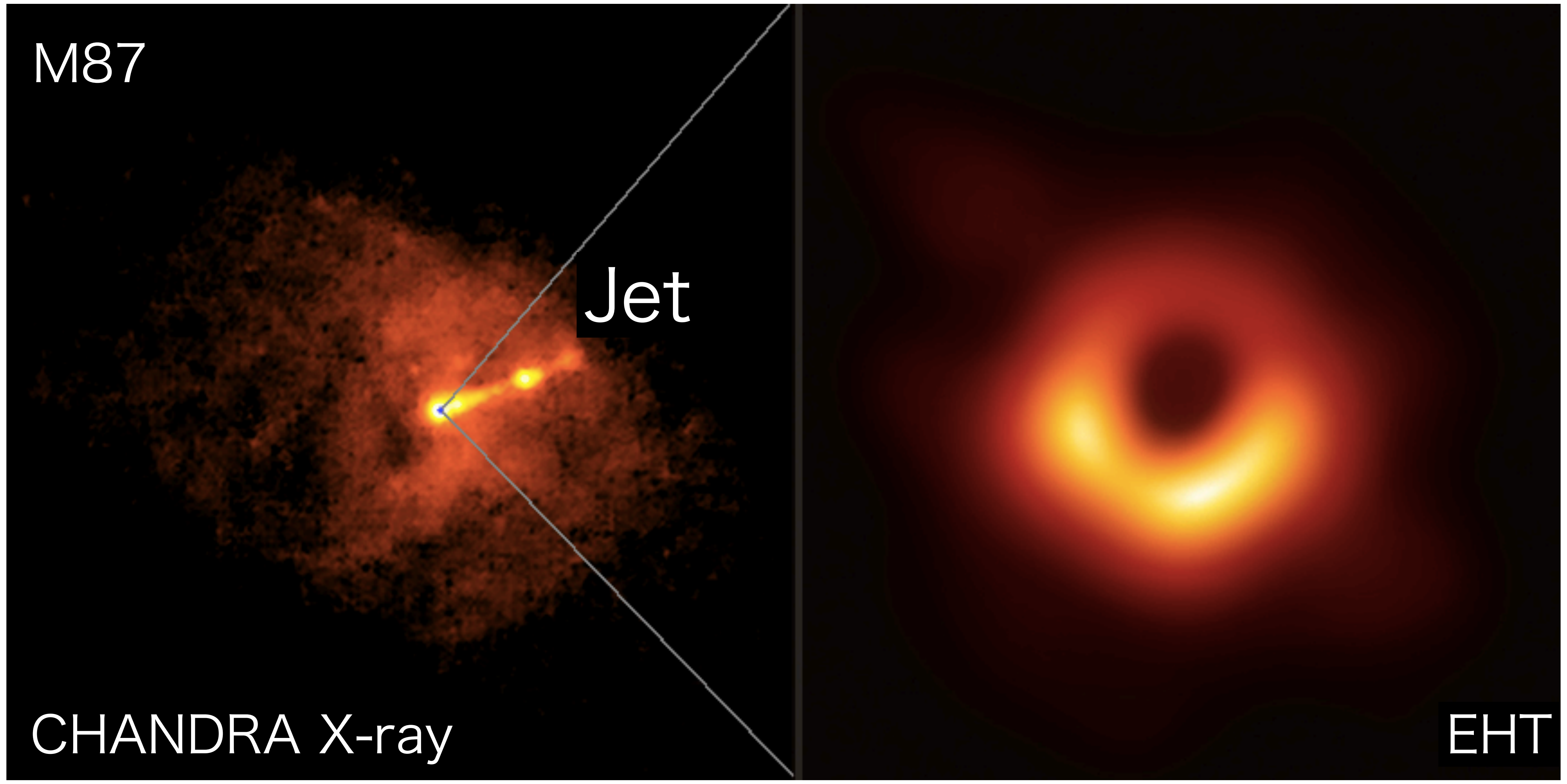

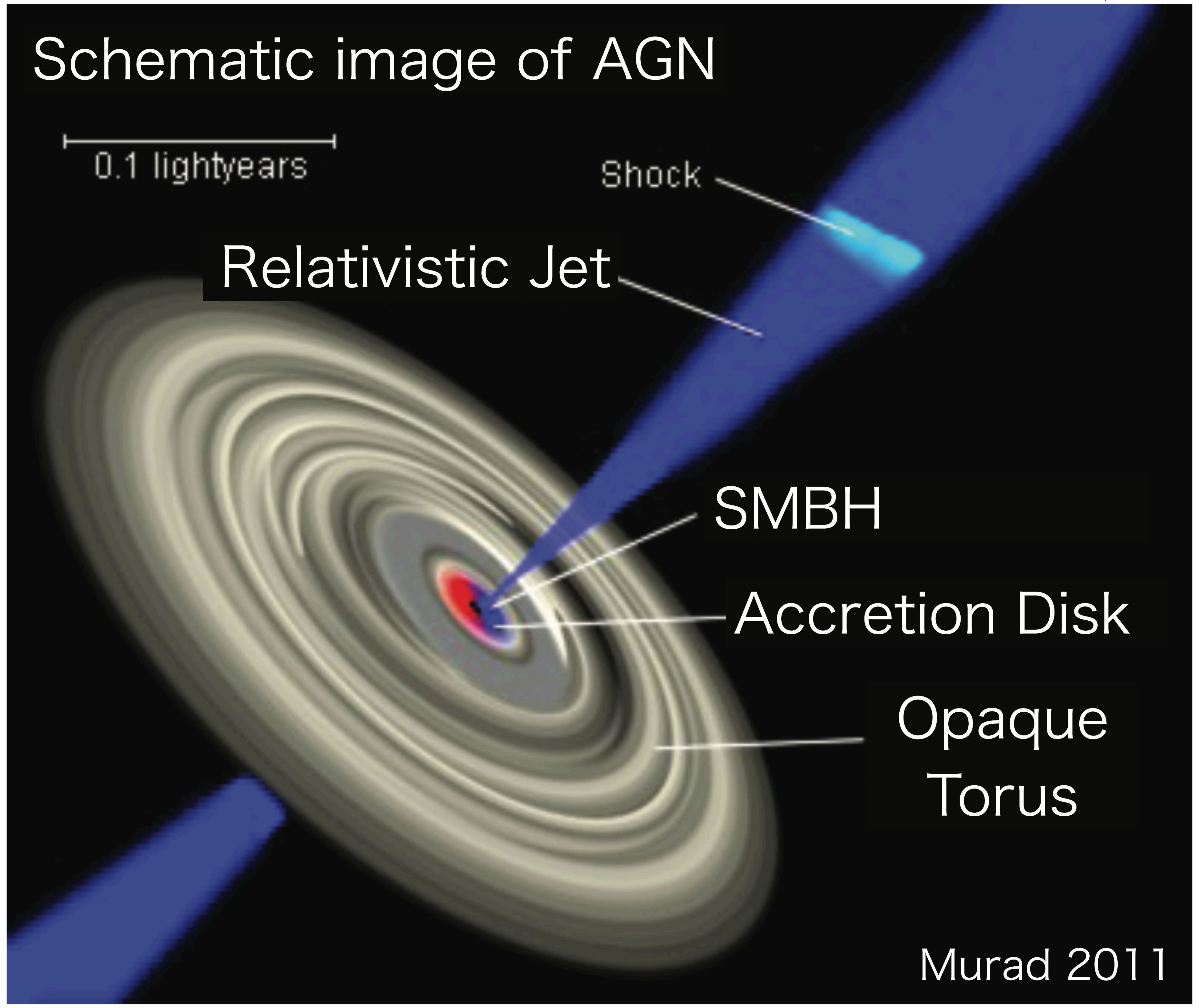

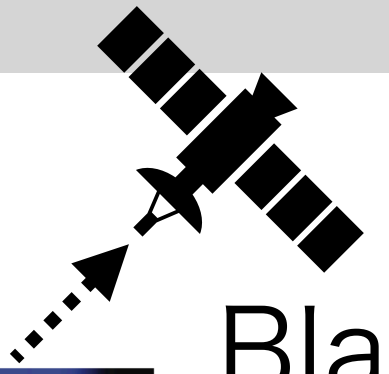

Blazar

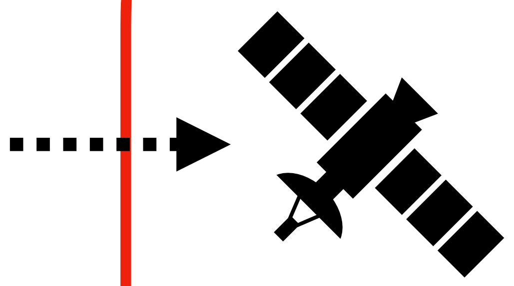

Radio Galaxy

- ✓ Radio-loud AGNs (10% of all AGNs) -> **Strong relativistic jet.**
- ✓ **GeV-TeV gamma-rays** are observed in nearby some radio galaxies.

Gamma-ray Observation

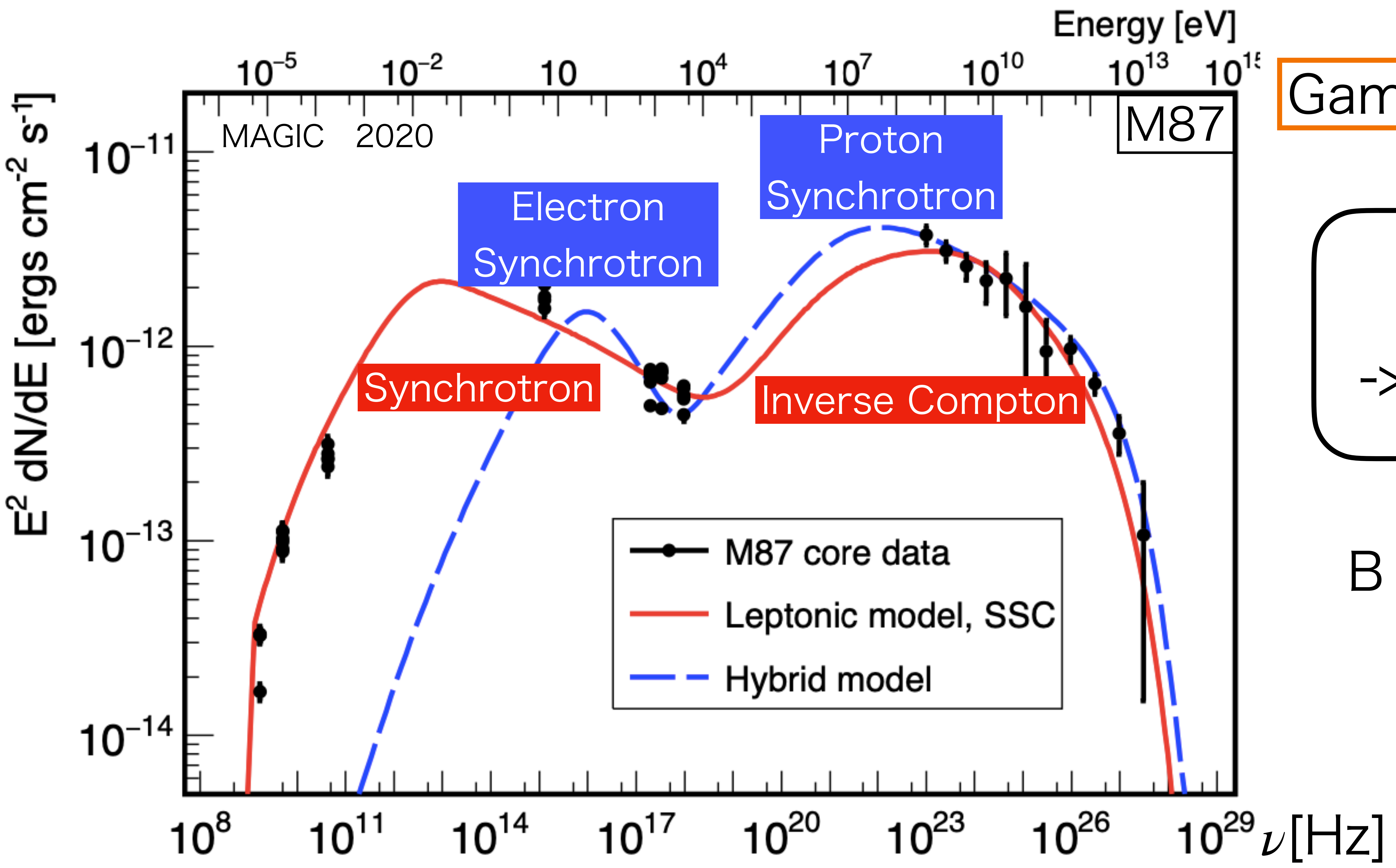

Gamma-ray Emission region…**Unknown**

Jet model

Broadband photons
-> Synchrotron + Inverse Compton

B fields by the spectral fitting(~mG)

^ MAGIC 2020

B fields by the radio image(~G)

Hadronic emission from the Magnetically Arrested Disks (MADs) is proposed. Kimura & Toma 2020

Objective

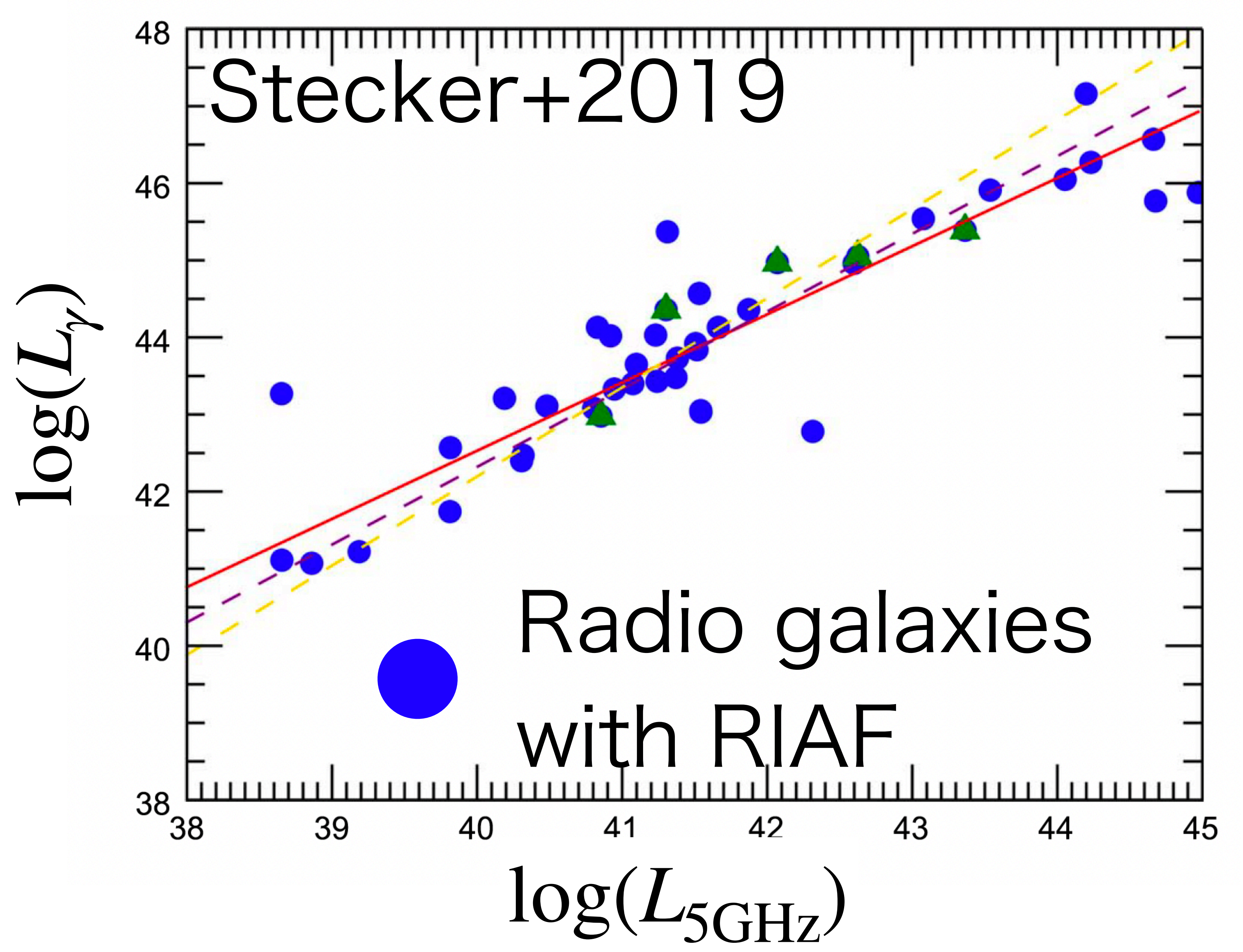

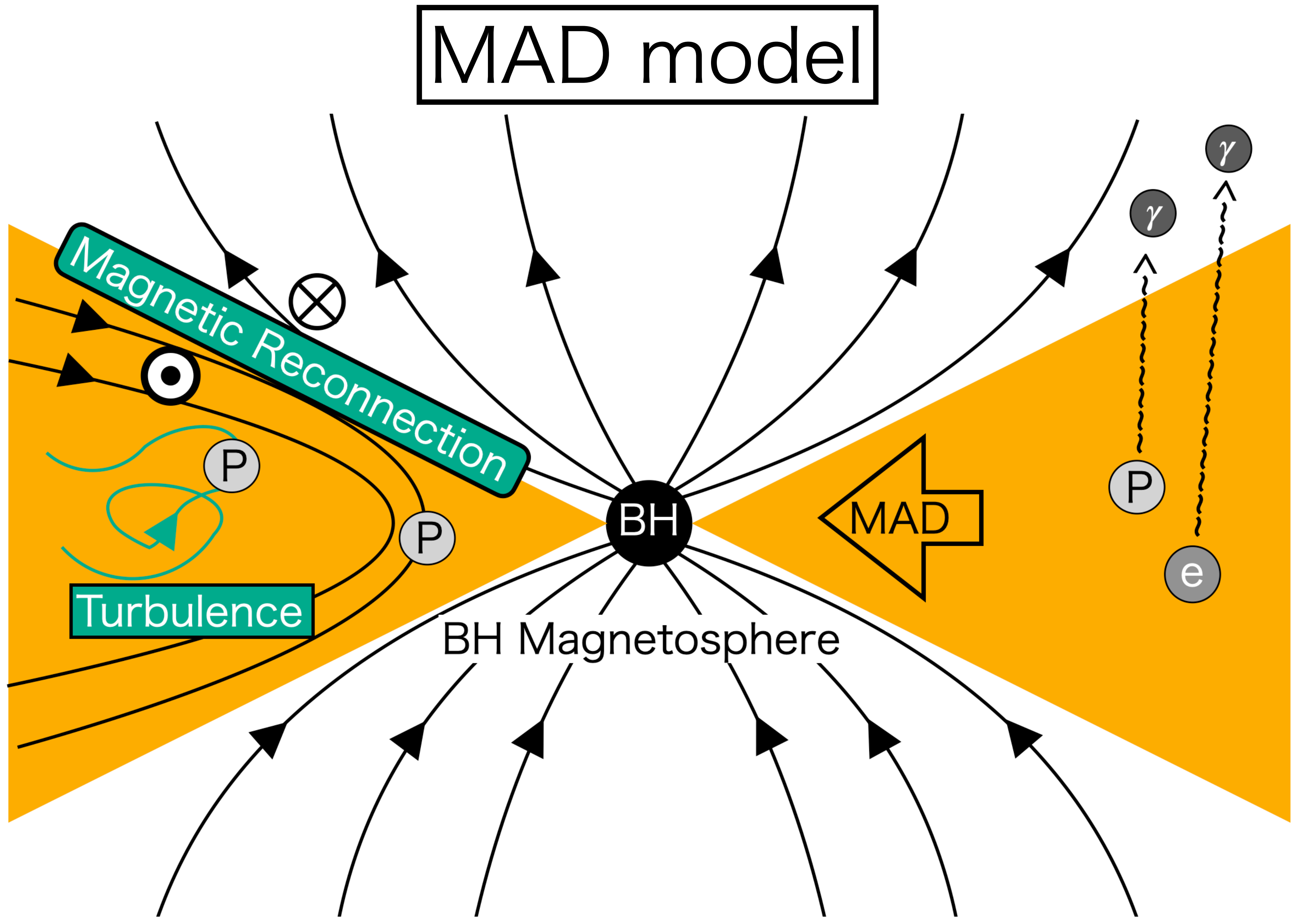

✔ Kimura & Toma (2020) shows that the MAD model can reproduce the GeV data of M87 and NGC 315. Kimura & Toma (2020)

✔ **The majority of GeV-detected radio galaxies are not explored yet.**

We investigate the characteristics of the radio galaxies that can be explained by the MAD model.

Magnetically Arrested Disks (MADs)

MHD simulation

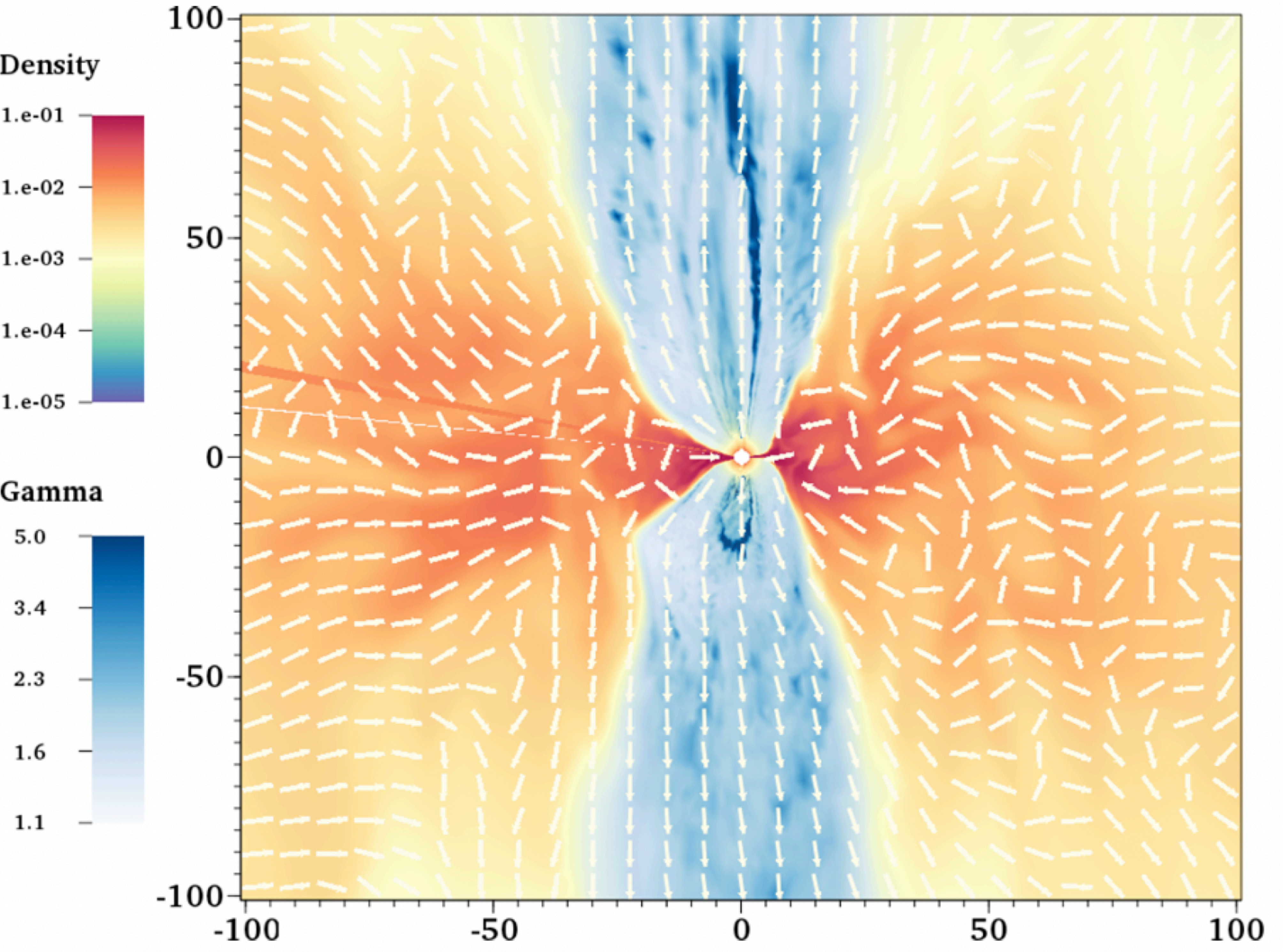

Sadowski et al. (2013)

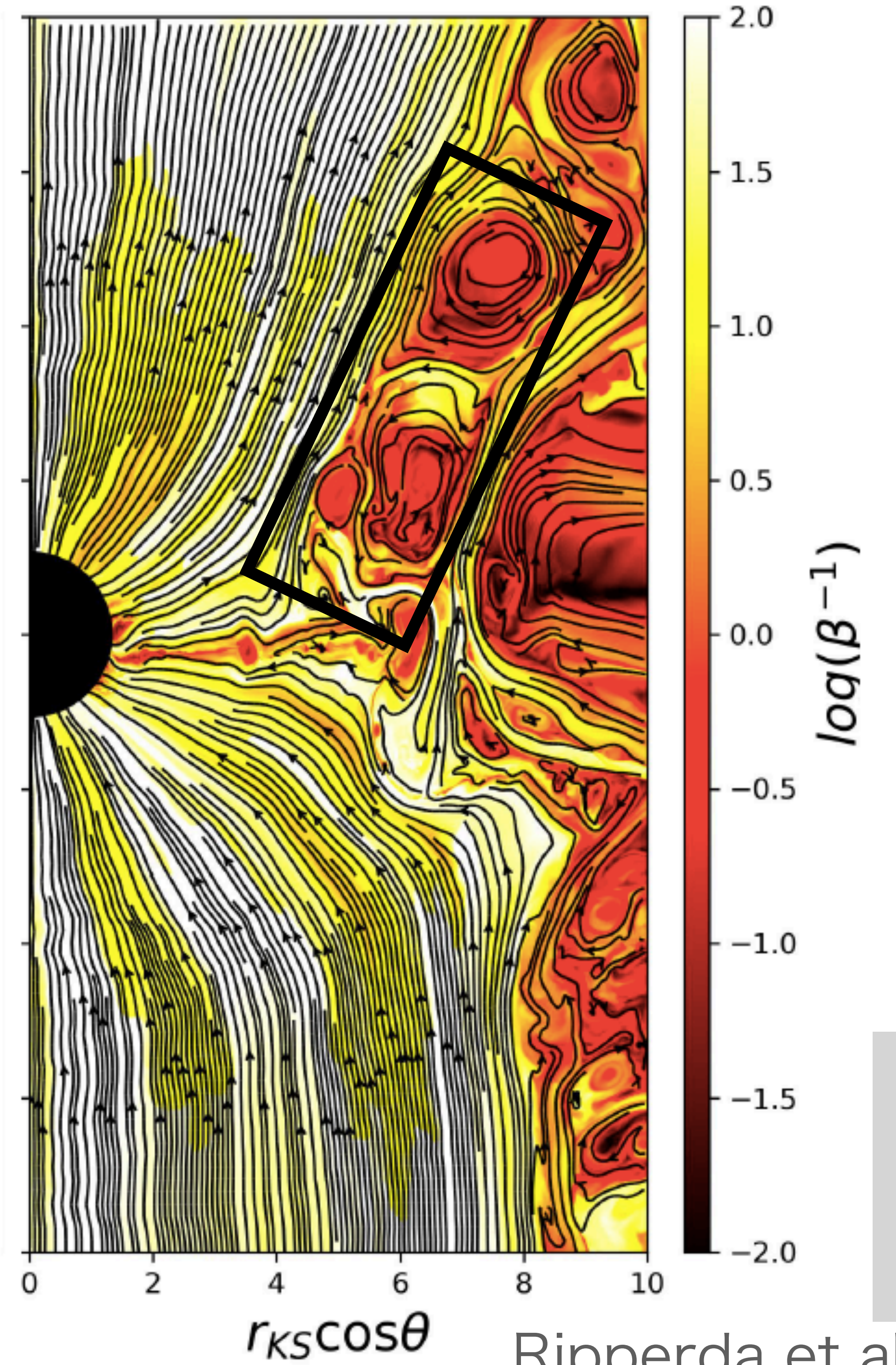

Ripperda et al. (2020)

Schematic image

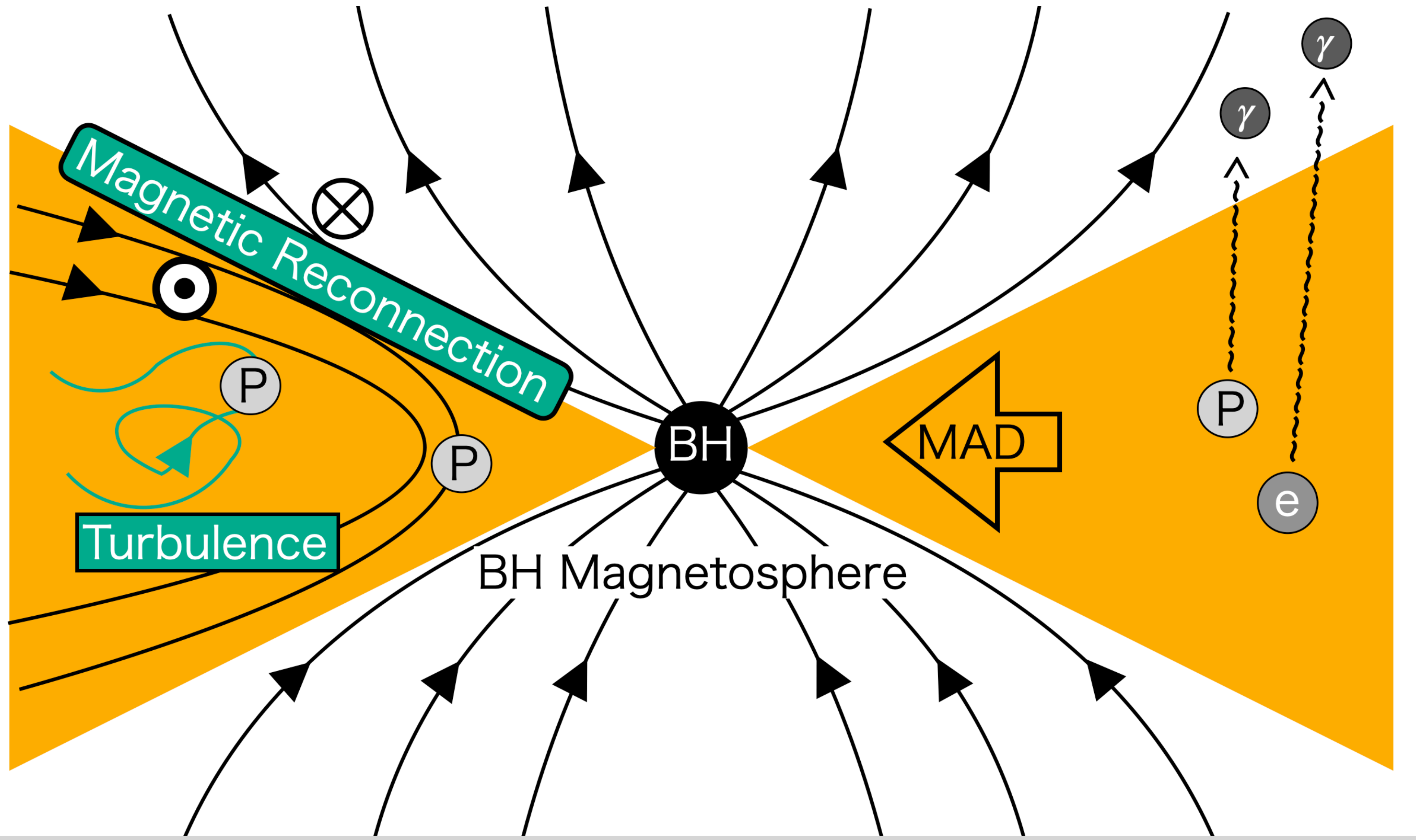

MADs
-> Strong magnetic fields.

Advantage of the MAD ▶

① Efficient jet production by the BZ process. Tchekhovskoy et al. (2011)

② B field by radio observation support MAD. Zamaninasab et al. (2014)

Efficient particle acceleration by the magnetic reconnection is expected.

Particle acceleration in MADs

Particle-in-Cell simulations

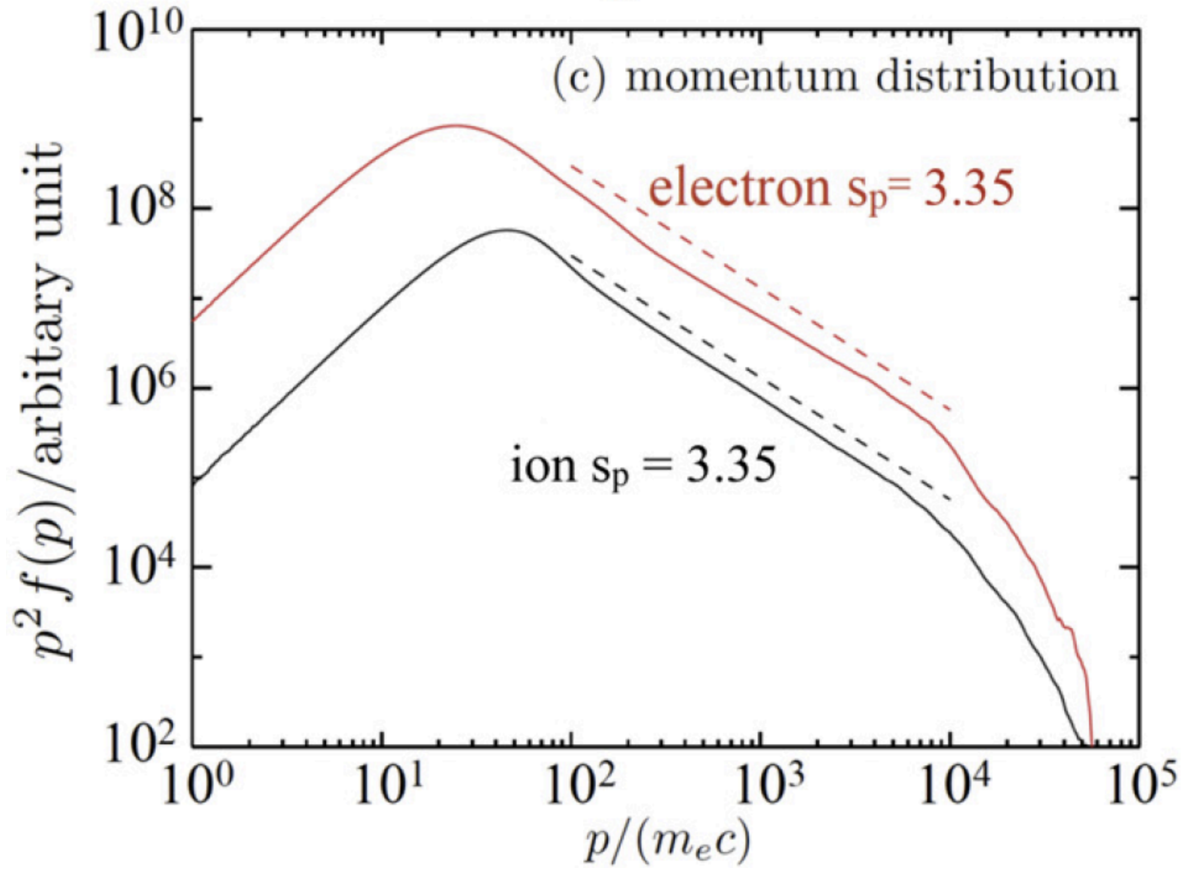

Guo et al. (2016)

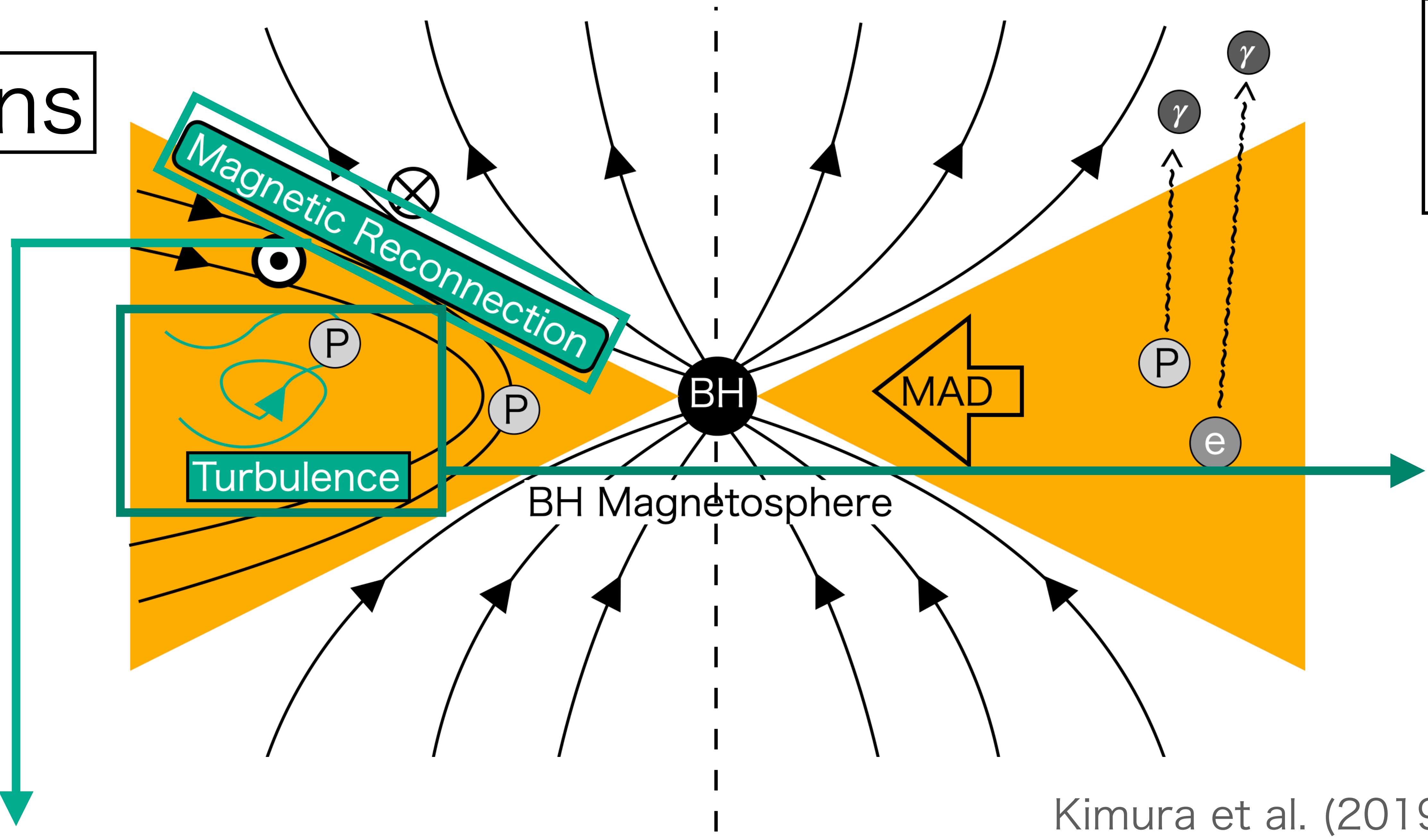

Test particle +
MHD simulations

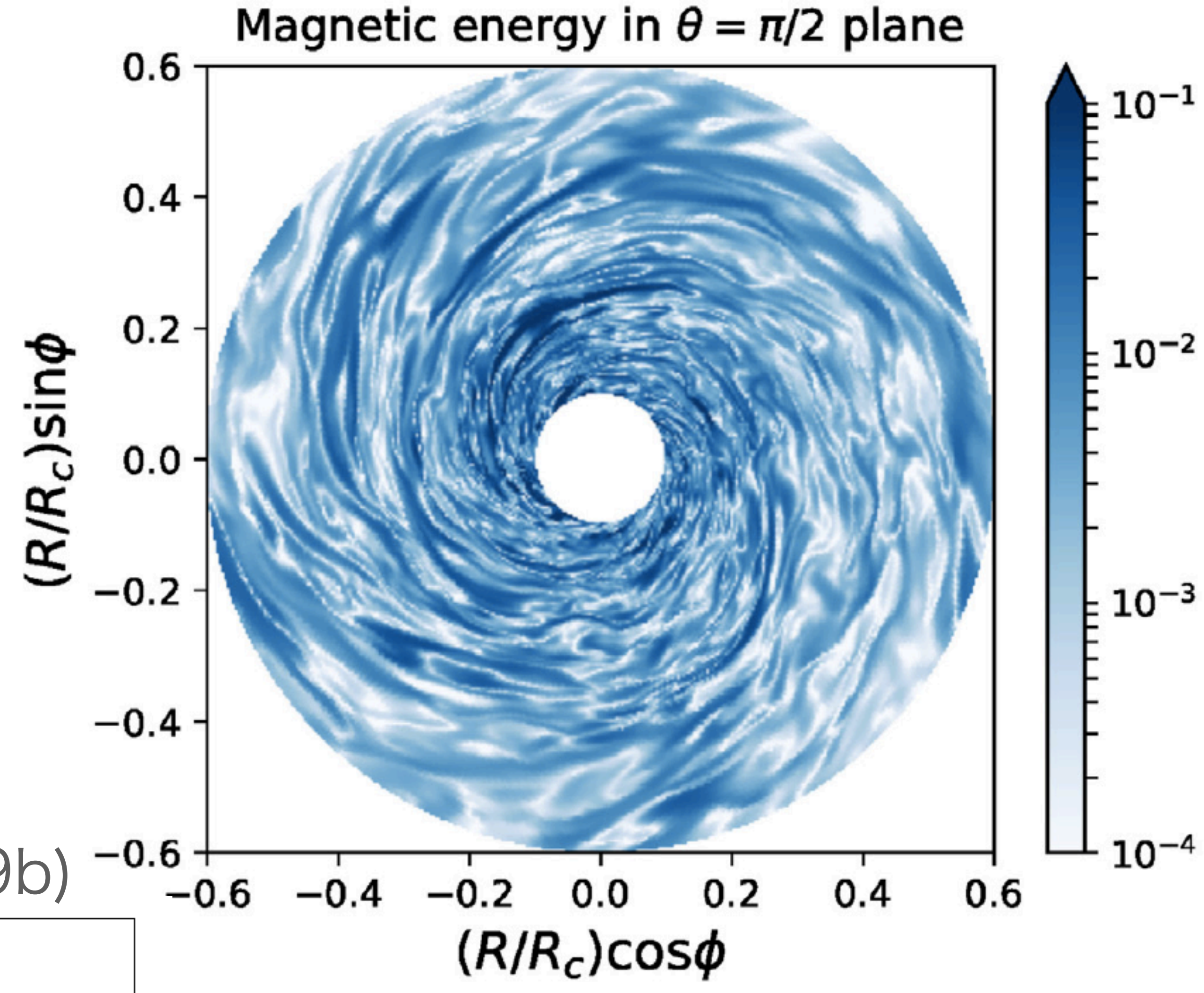

Kimura et al. (2019b)

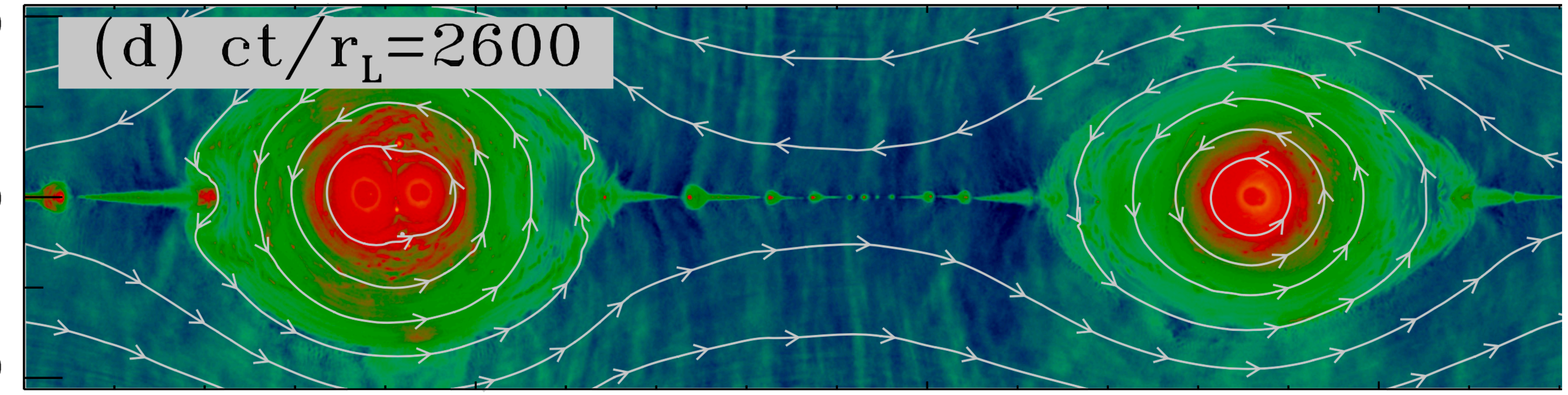

Petropoulou & Sironi 2018

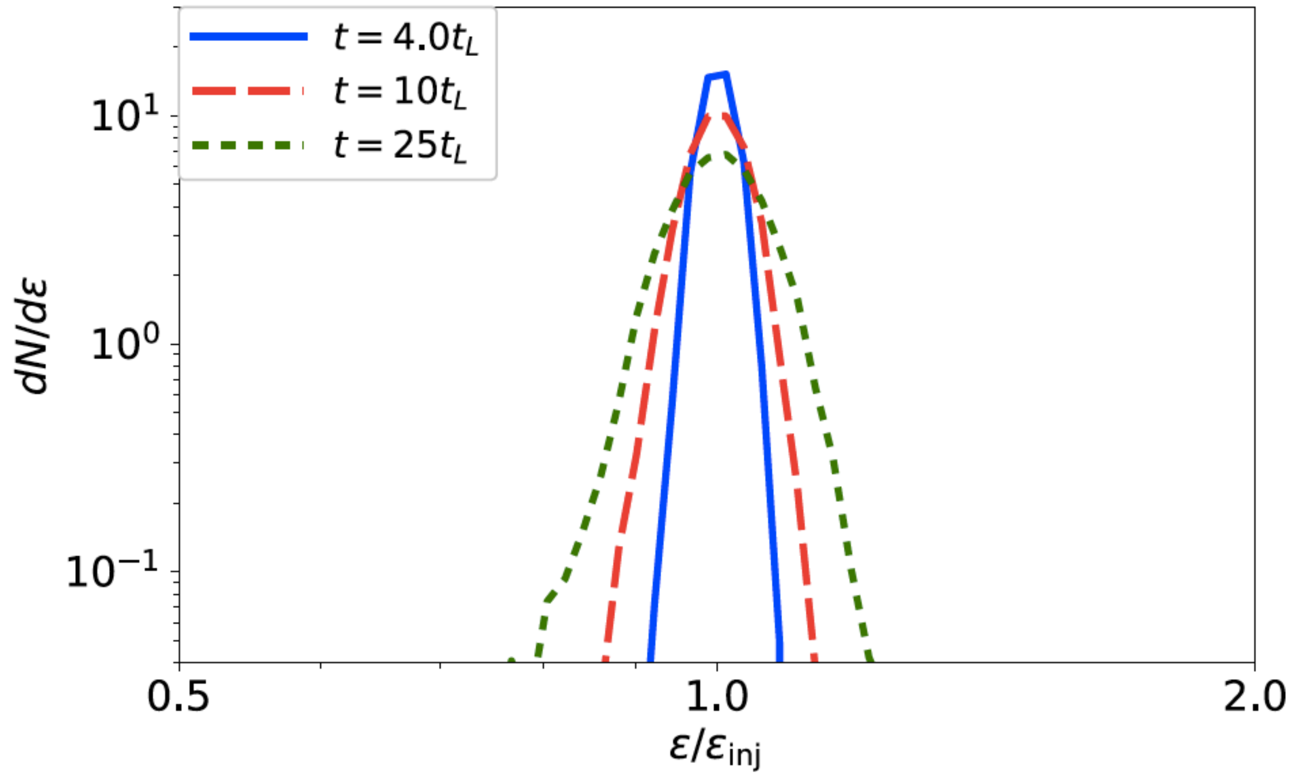

Kimura et al. (2019b)

MHD Turbulent

Magnetic reconnection or MHD turbulence accelerates the CRs.

MAD model

- Steady & one-zone approximation

- 5 particle species

Thermal electron | Primary electron | Primary proton

$p+\gamma \rightarrow p+e^{+}+e^{-}$ | $\gamma+\gamma \rightarrow e^{+}+e^{-}$

Synchrotron radiation produce the broadband photons.

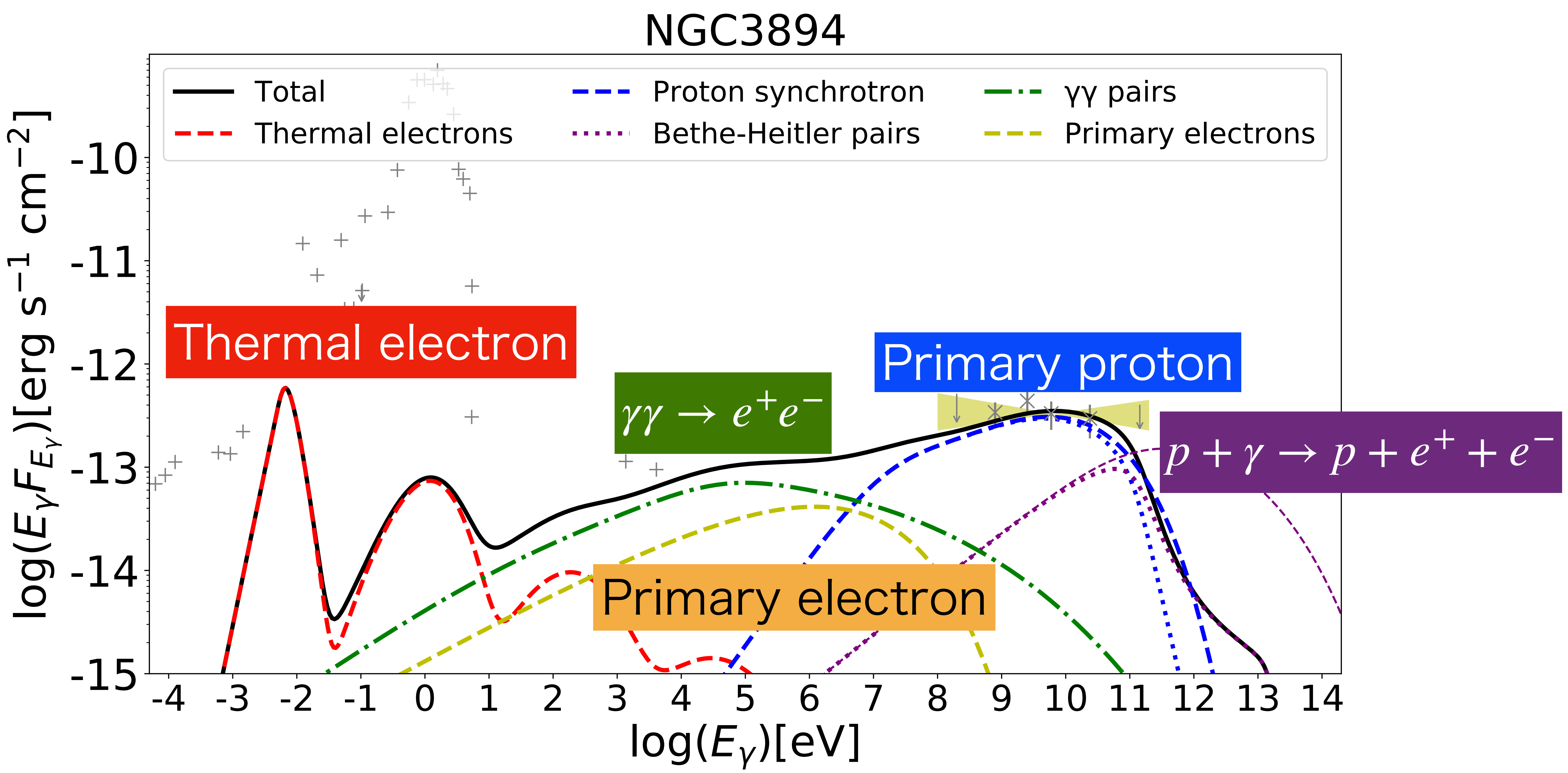

- Equation of continuity in energy space

$$-\frac{d}{dE_i}\left(\frac{N_{E_i}E_i}{t_{i,\mathrm{cool}}}\right) = \dot{N}_{E_i,\mathrm{inj}} - \frac{N_{E_i}}{t_{\mathrm{esc}}}$$

Cooling Injection Escape

- Cooling time $t_{i,\mathrm{cool}}$
- Escape time t_{esc}

Injection Term

$$\dot{N}_{E_{i,\mathrm{inj}}} = \dot{N}_0\left(\frac{E_i}{E_{i,\mathrm{cut}}}\right)^{-s_{\mathrm{inj}}} \exp\left(-\frac{E_i}{E_{i,\mathrm{cut}}}\right)$$

Timescale of the MAD model

■ Cooling time $t_{i,\mathrm{cool}}$

Synchrotron Radiation

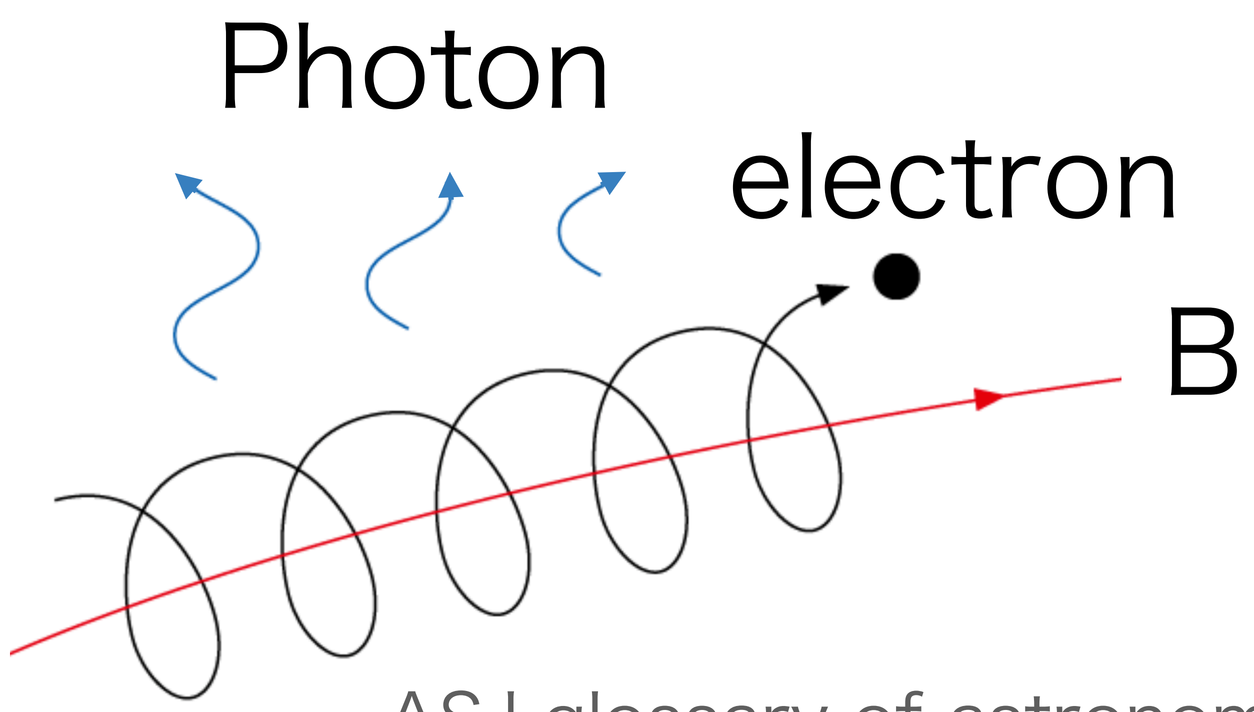

ASJ glossary of astronomy

Proton-photon interaction

Bethe-Heitler process

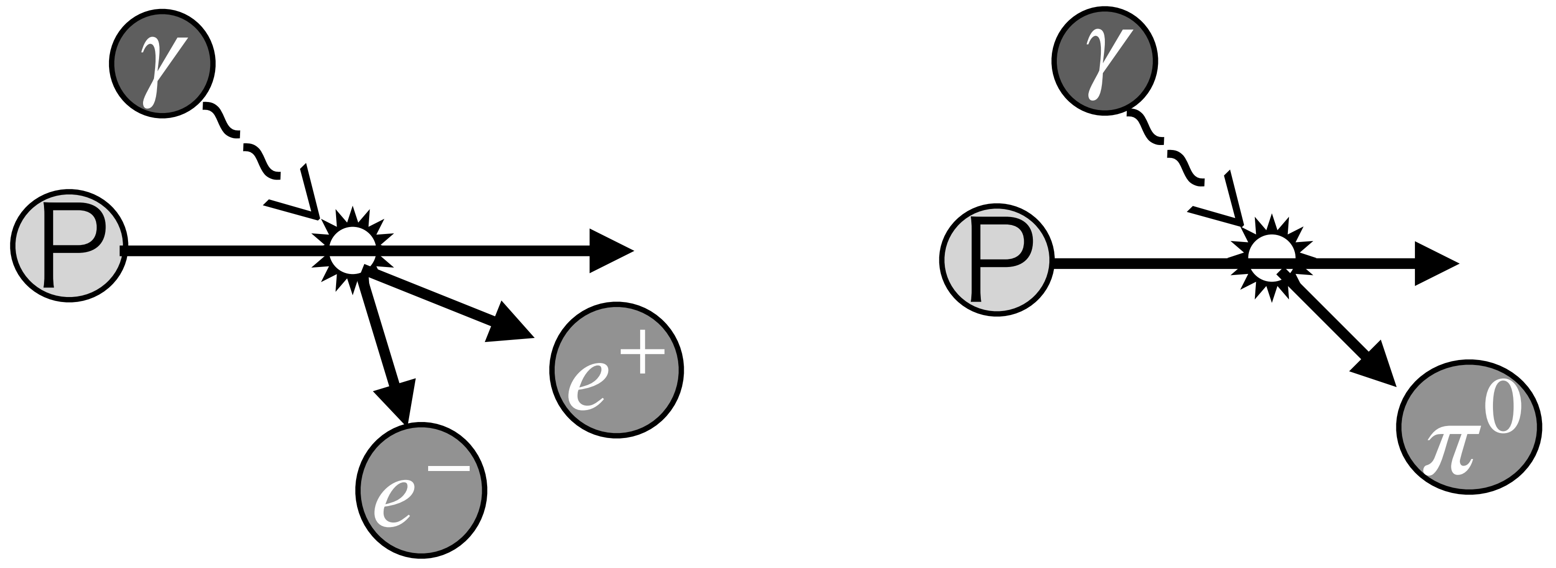

$p + \gamma \rightarrow p + e^+ + e^-$ $\quad$ $p + \gamma \rightarrow p + \pi^0$

pp collision

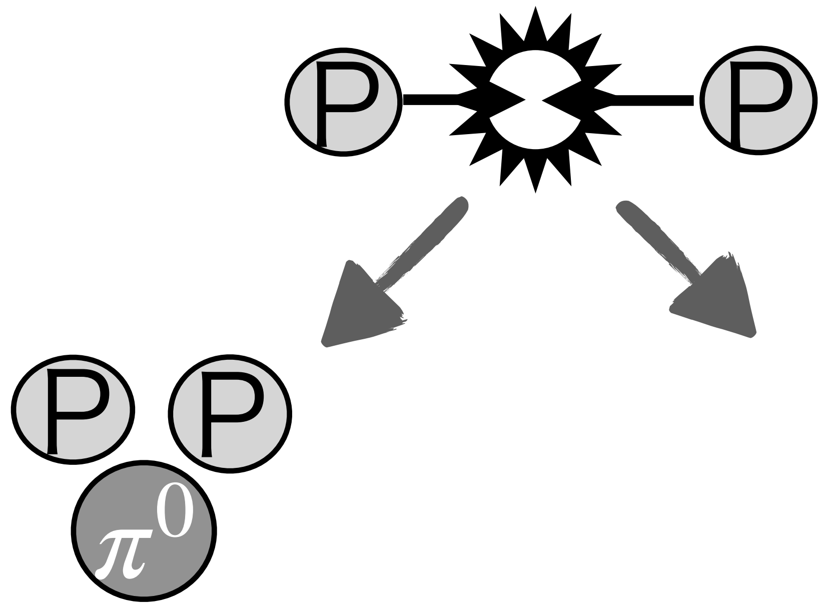

$p + p \rightarrow p + p + \pi^0$ $\quad$ $p + p \rightarrow p + n + \pi^+$

■ Escape time t_{esc}

(i) Infall

(ii) Diffusion

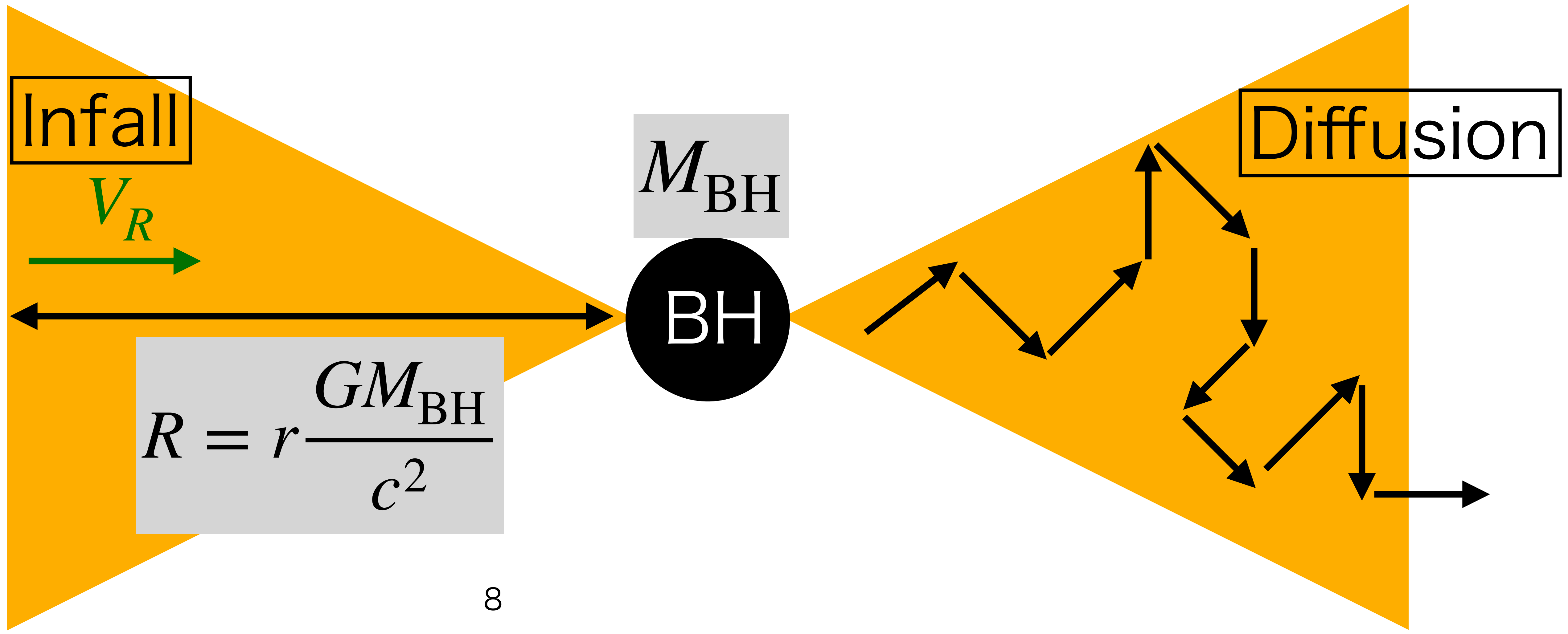

Pick out process

GeV gamma-rays
-> Synchrotron radiation by the primary protons.

Fermi 4LAC-DR2 catalog

We picked out the
15 GeV-loud radio galaxies.

Apply the MAD model to the
15 GeV-loud radio galaxies.

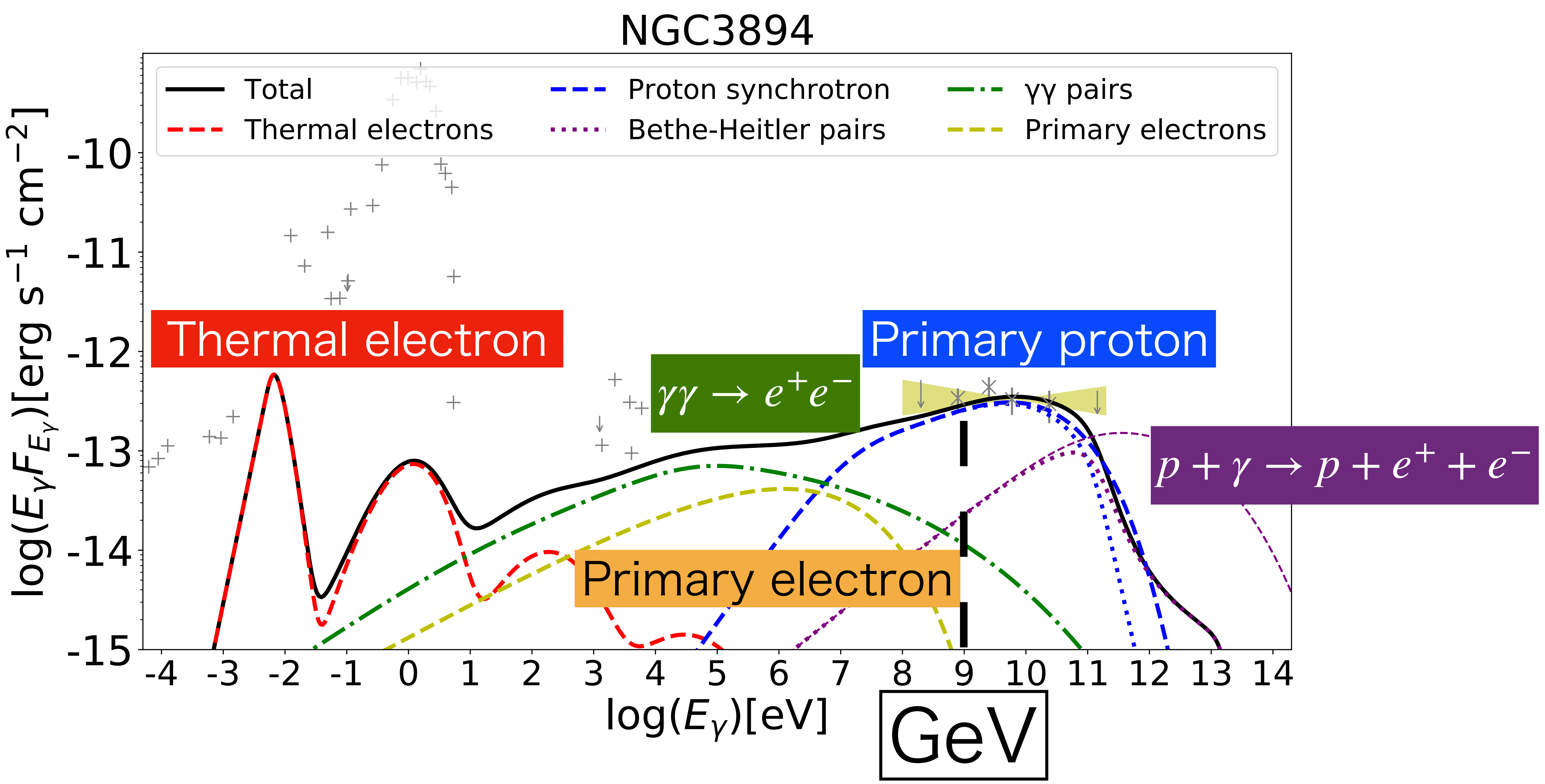

We also apply the MAD model to **Sgr A***

Results

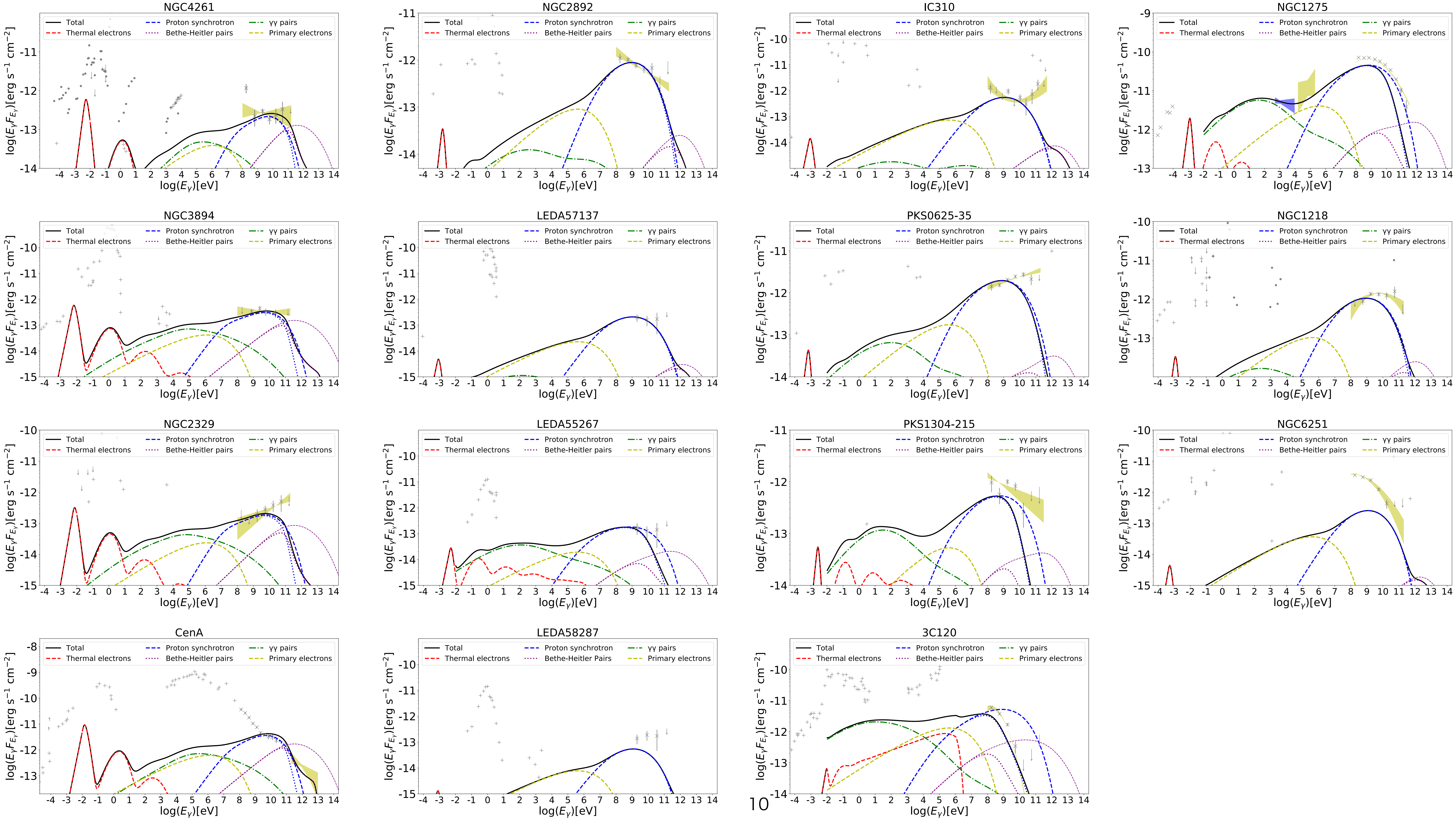

NGC4261
NGC2892
IC310
NGC1275
NGC3894
LEDA57137
PKS0625-35
NGC1218
NGC2329
LEDA55267
PKS1304-215
NGC6251
CenA
LEDA58287
3C120
Total
Thermal electrons
Proton synchrotron
Bethe-Heitler pairs
γγ pairs
Primary electrons
$\log(E_\gamma F_{E_\gamma})$[erg s^{-1} cm^{-2}]
$\log(E_\gamma)$[eV]

Classification of the results

We classify the result into three; Excellent, Good, Bad

★ Excellent

● Good

ex)

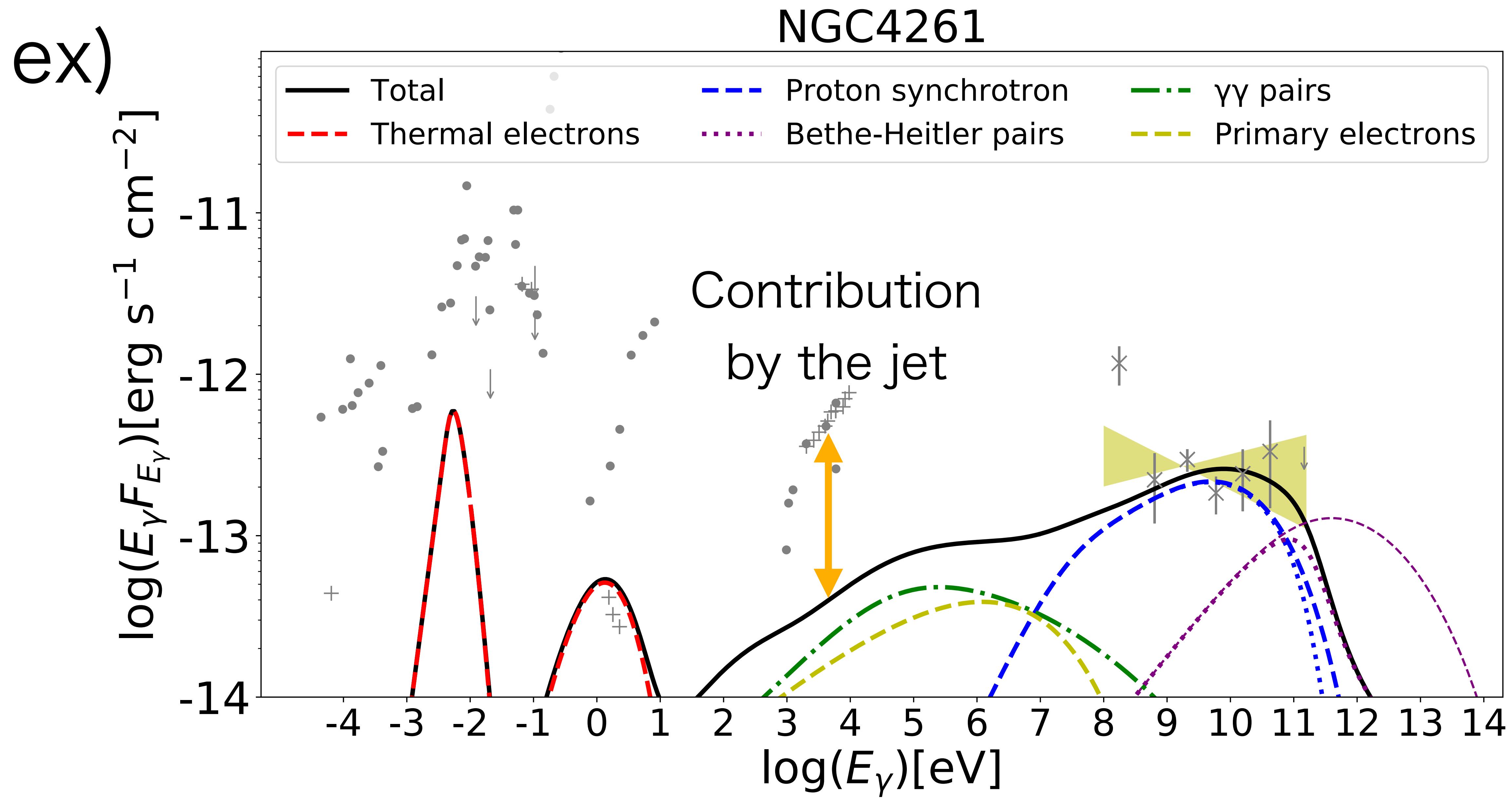

ex)

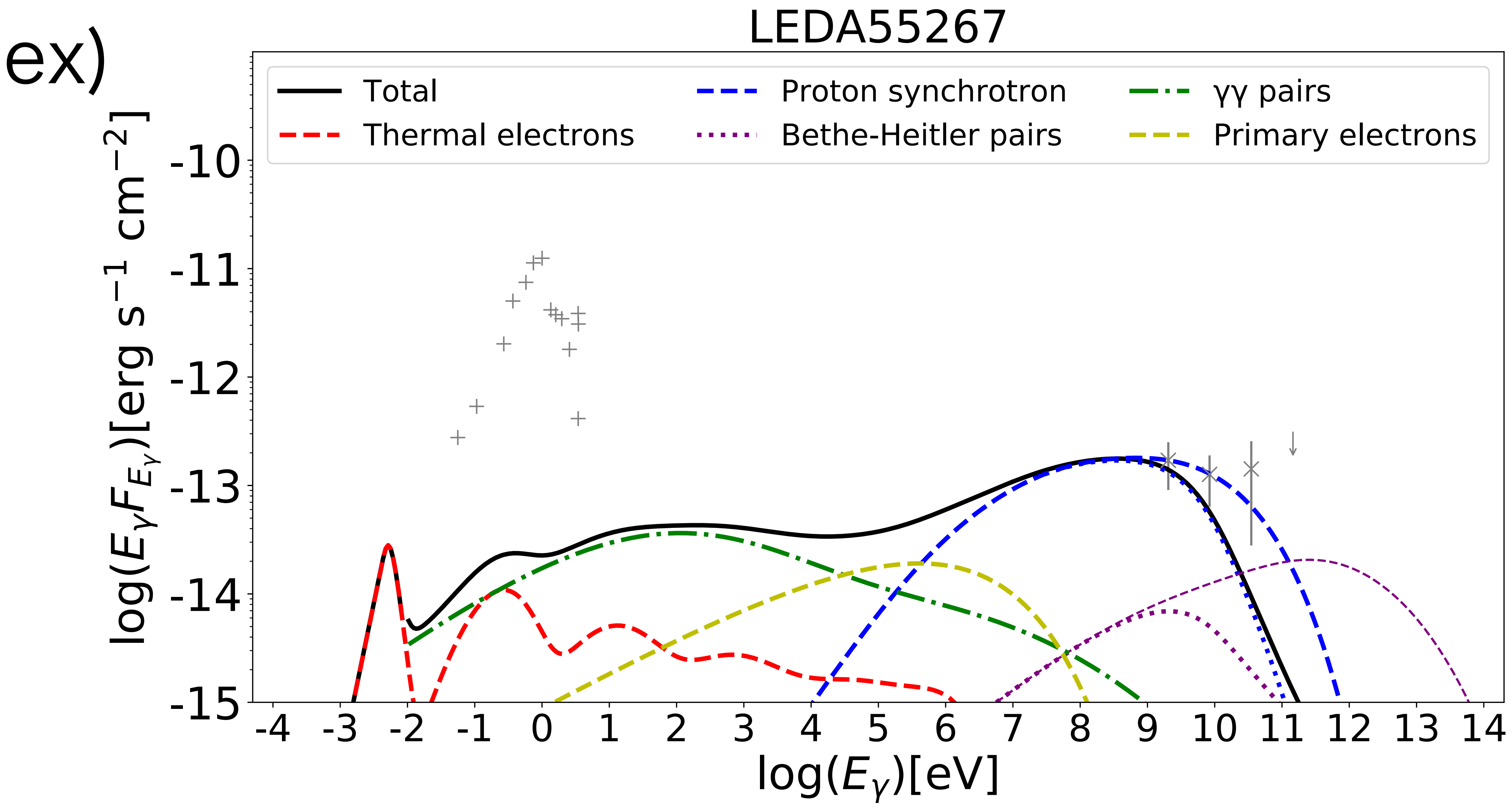

Excellent: Changing only the $\dot{m}$.

Fiducial parameter set:

$r = 10,\ \alpha = 0.3,\ \beta = 0.1,\ \epsilon_{\rm NT} = 0.33,\ \epsilon_{\rm dis} = 0.15,\ \eta = 5,\ s_{\rm inj} = 1.3$

Good: $r = 30$ + Three times $M_{\rm BH}$

Classification of the results

We classify the result into three; Excellent, Good, Bad

✕ Bad

ex)

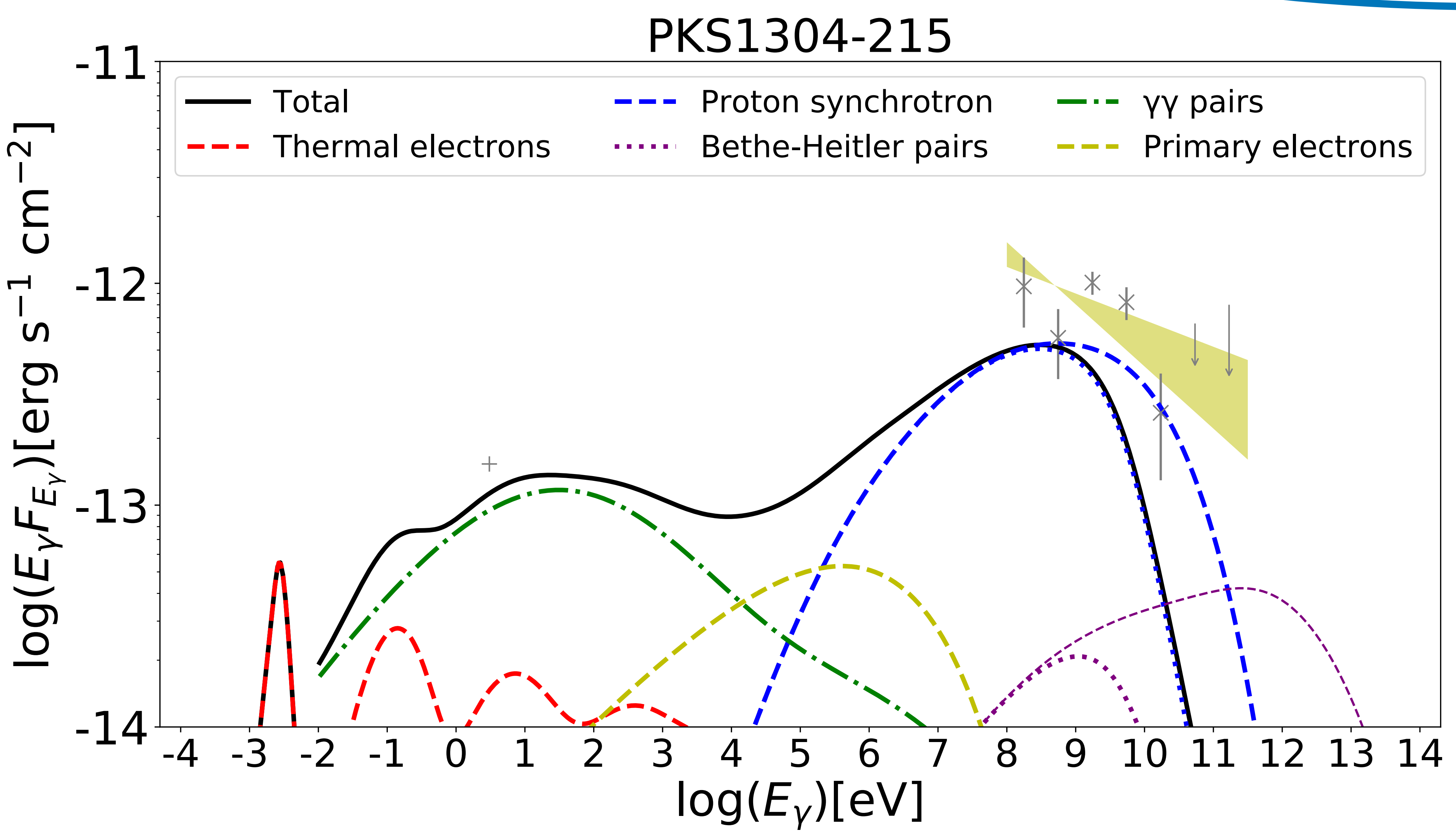

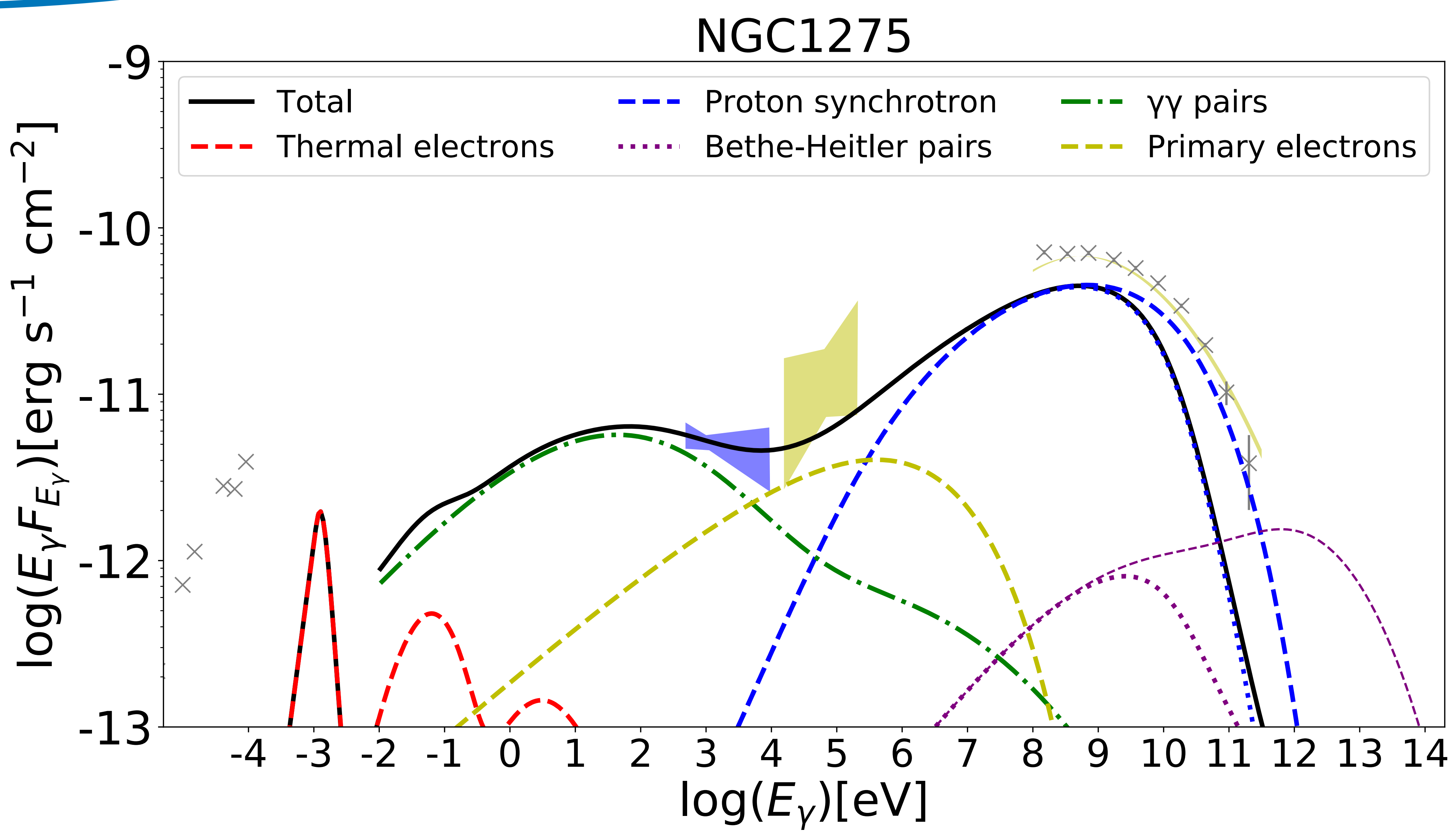

$\gamma\gamma \rightarrow e^+e^-$ absorbs the GeV gamma-rays.

-> Cut-off below the GeV

Exceeds the X-ray data.

Mass to accretion rate

$\dot{m} < 10^{-3}$

(Lower than the 0.1% of the Eddington rate)

-> We can reproduce the GeV data

↕

$\dot{m} > 10^{-3}$

-> GeV gamma-rays are absorbed by the $\gamma + \gamma \rightarrow e^{+} + e^{-}$.

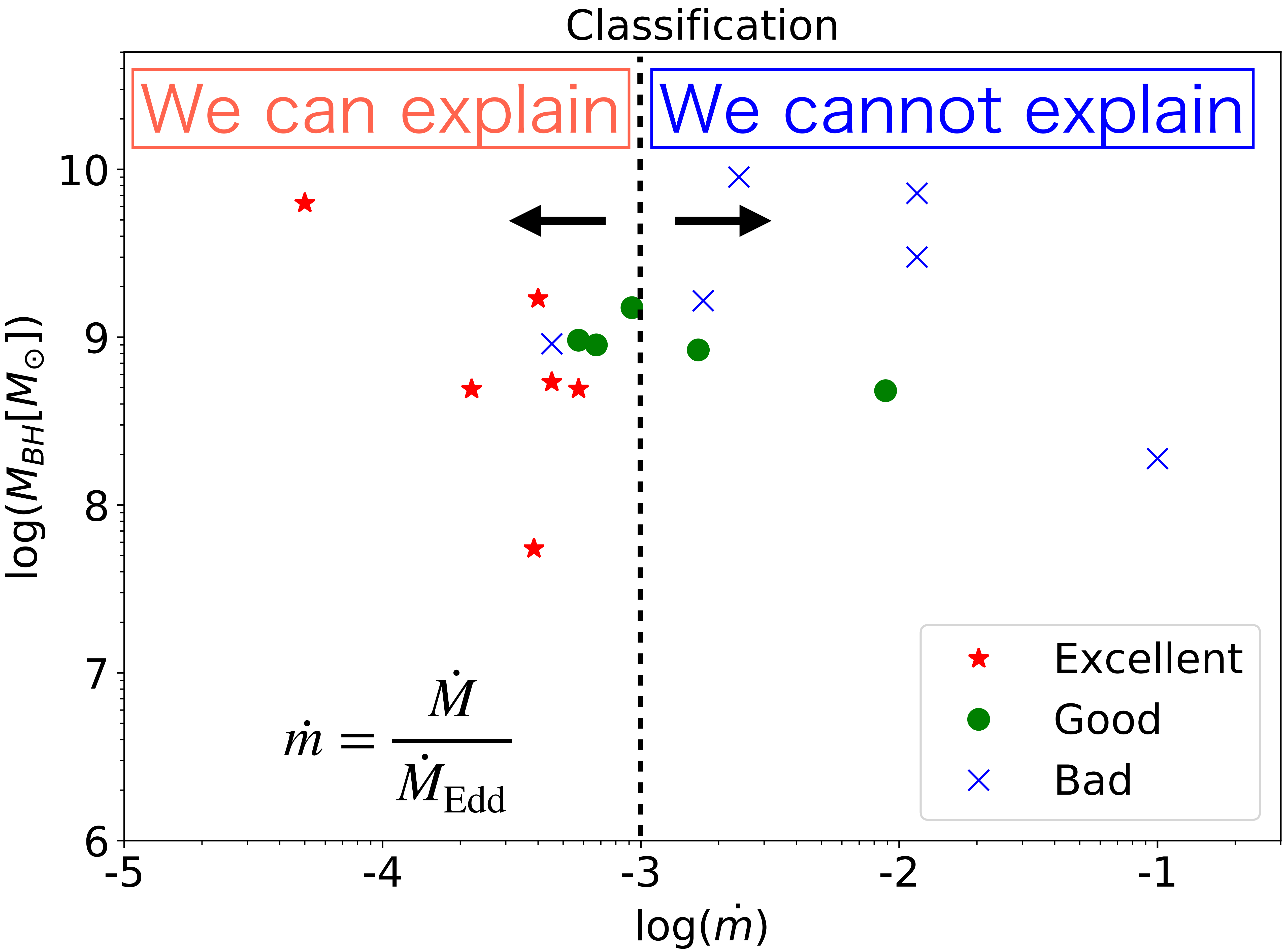

★ We can reproduce the data by only changing the $\dot{m}$

● We can reproduce the GeV data with changed parameters.

✕ We cannot reproduce the GeV data.

Sgr A*

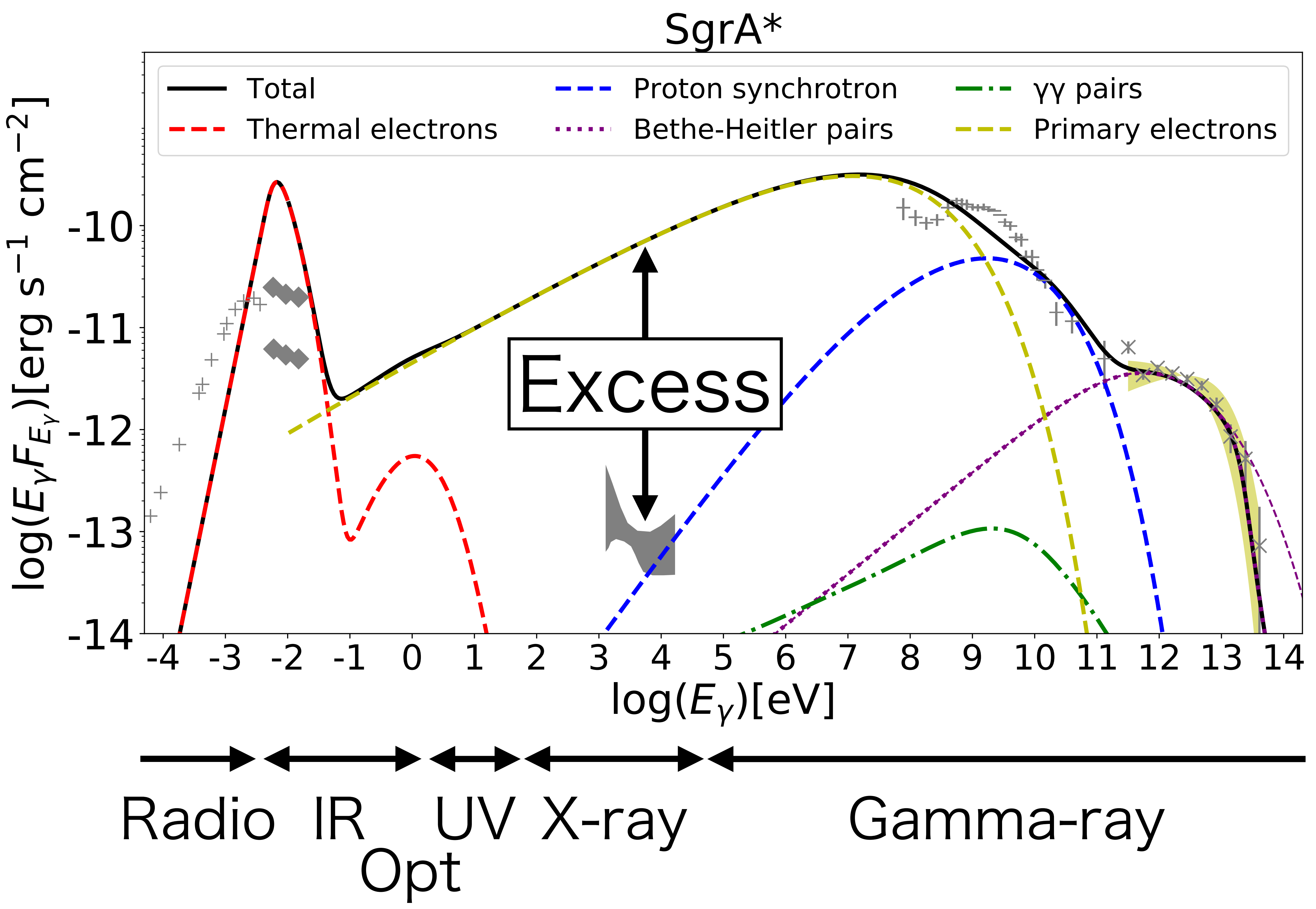

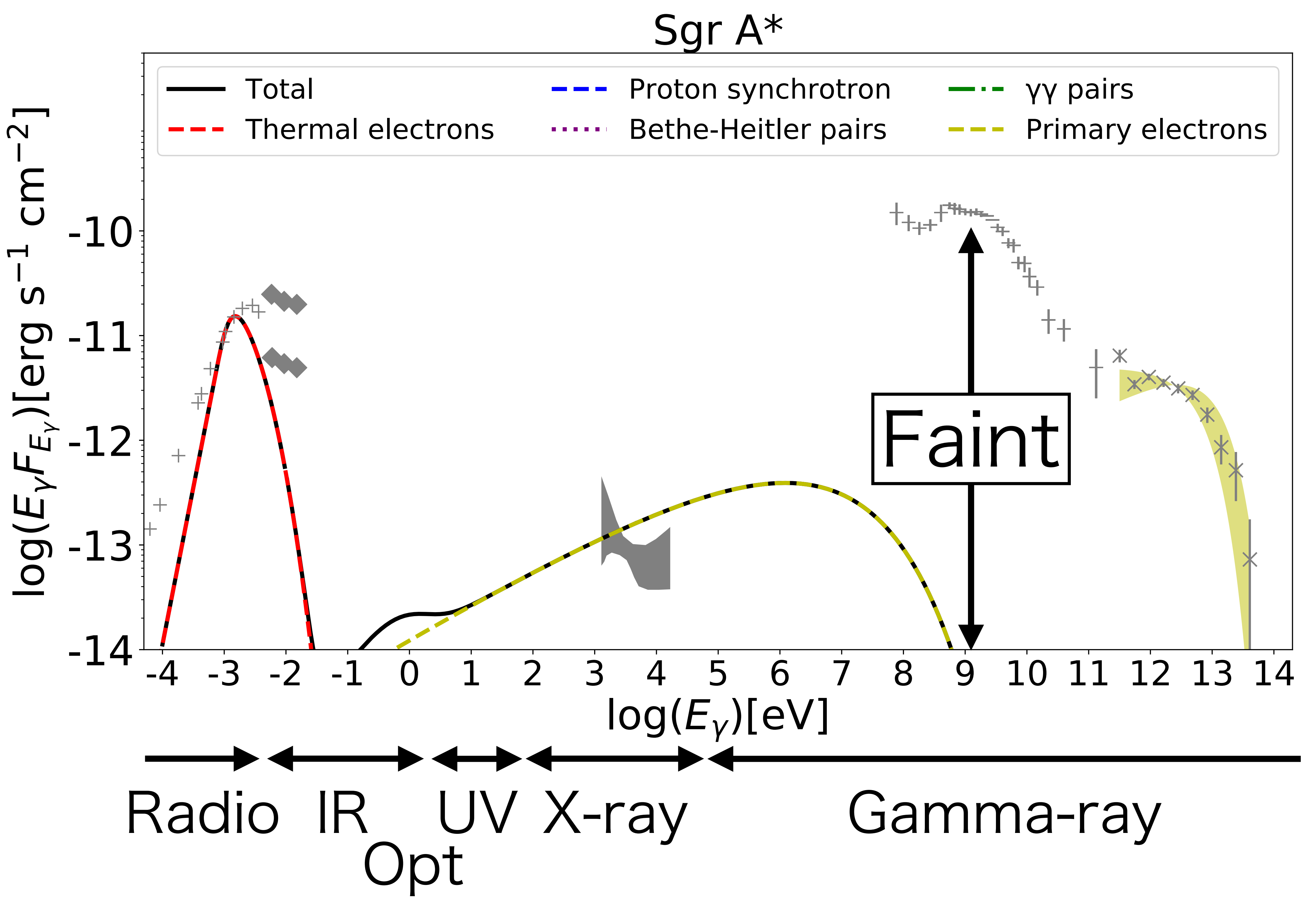

$\dot{m}$ adjusted to the GeV data

-> Exceed the Radio, X-ray data.

$\dot{m}$ adjusted to the Radio and X-ray data.

-> We cannot reproduce the GeV data.

The origin of the GeV gamma-rays is not the MAD of Sgr A*.

Summary

- ✔ Hadronic emission from MADs is proposed as the one possible scenario of the gamma-ray origins, and the majority of the GeV detected radio galaxies are not explored yet.
- ✔ We investigate the characteristics of the radio galaxies explained by the MAD model by applying the 15 GeV-loud radio galaxies.
- ✔ We find that the **MAD model can reproduce the GeV data if the $\dot{m}$ is lower than the 0.1% of the Eddington rate.**
- ✔ **We find that the source of the gamma rays observed at the Galactic center is not Sgr A*, but other objects in the Galactic center.**

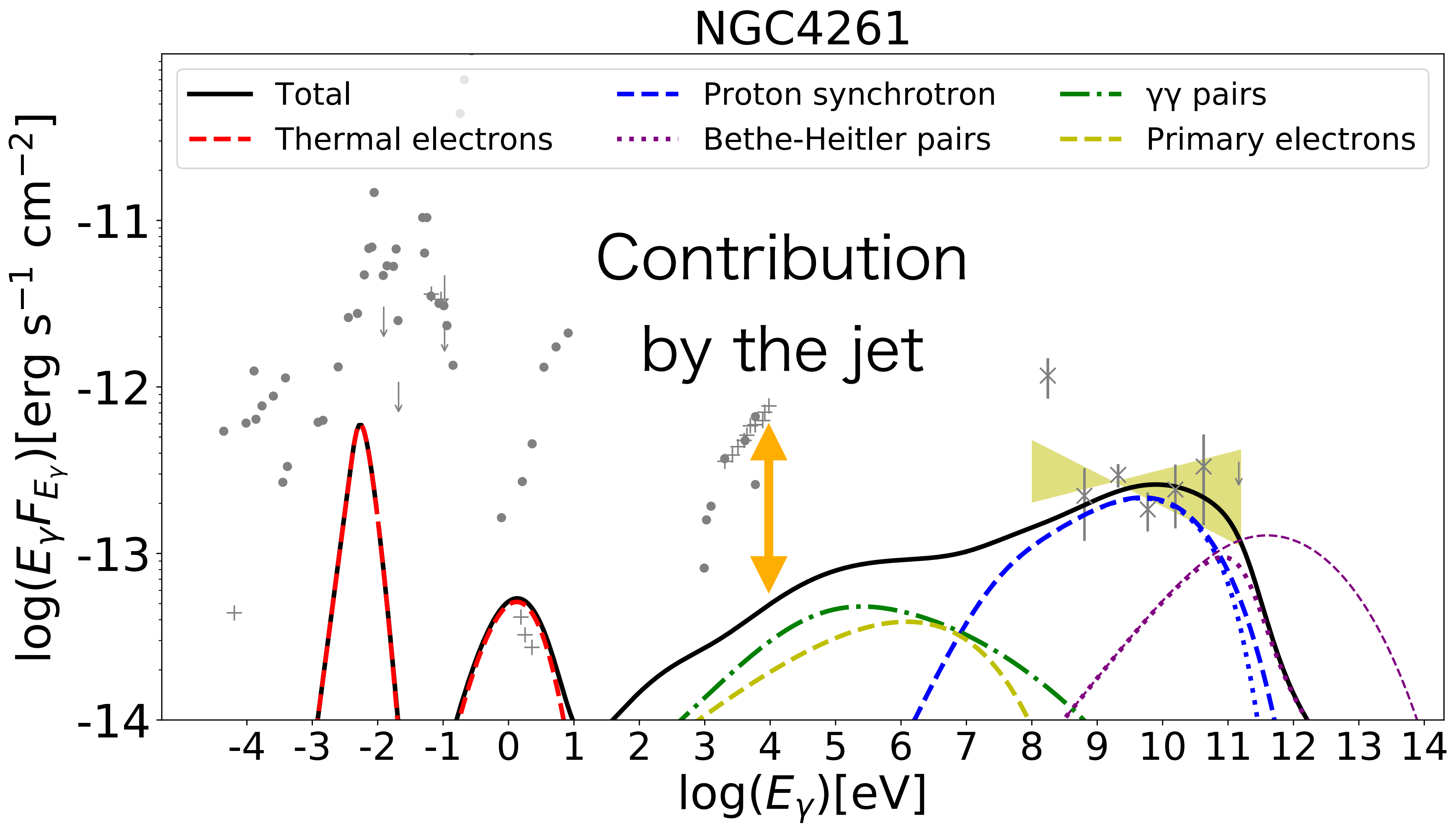

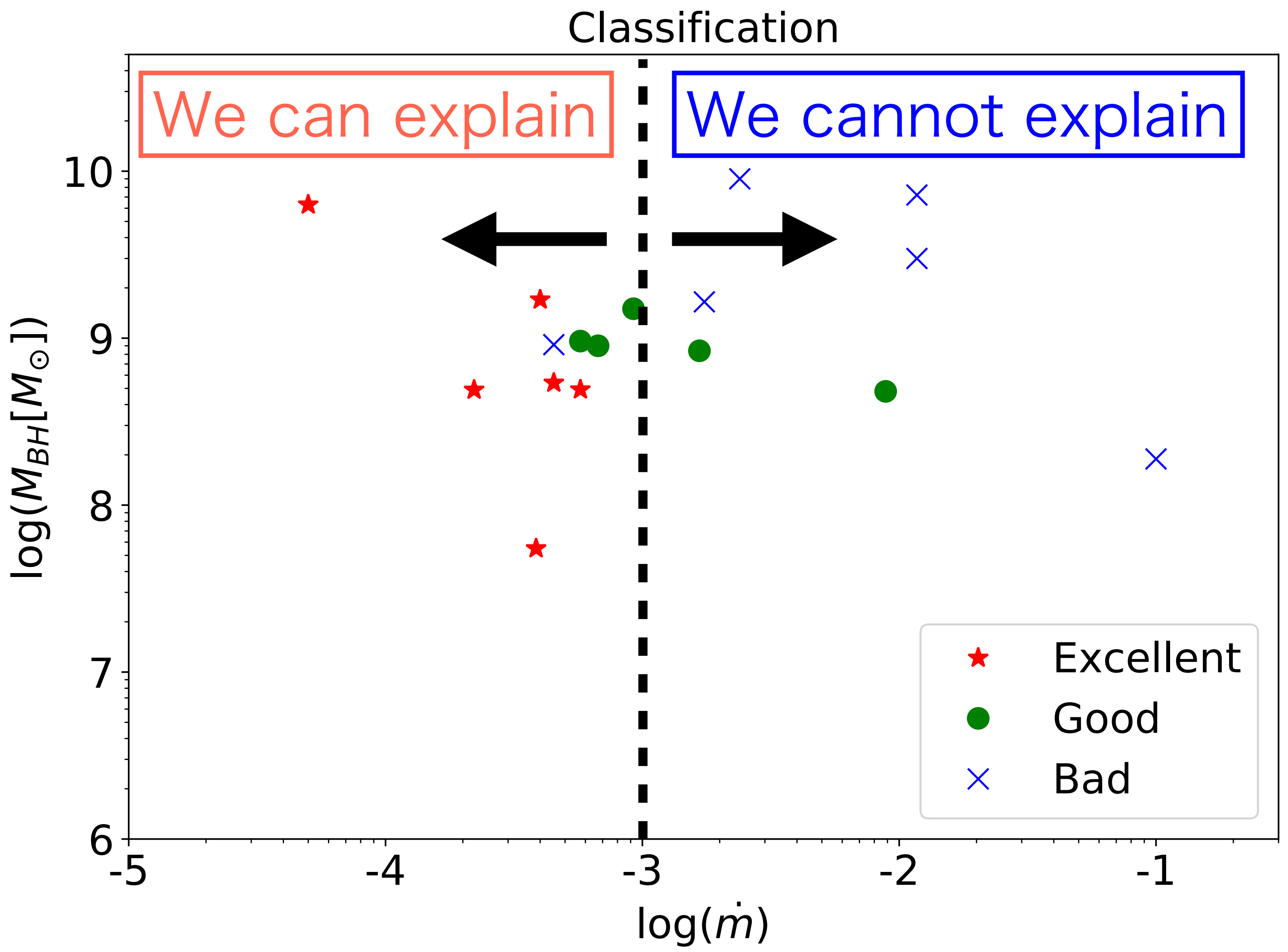

Thank you for listening

BackUp Slide

Accretion disks

Standard disks

High $\dot{M}$ → High ρ → High photon energy
High ρ → Low thermal energy
→ Geometrically thin, optically thick, cold accretion disk

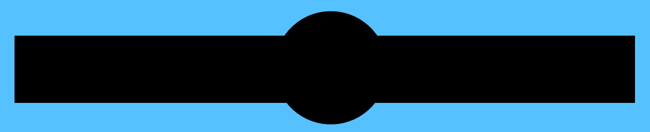

MAD: **Accretion flow with strong magnetic field**

Magnetically Arrested Disk

RIAF

Radiatively Inefficient Accretion Flow

Low $\dot{M}$ → Low ρ → Low photon energy
Low ρ → High thermal energy
→ Geometrically thick, optically thin, hot accretion flow

H
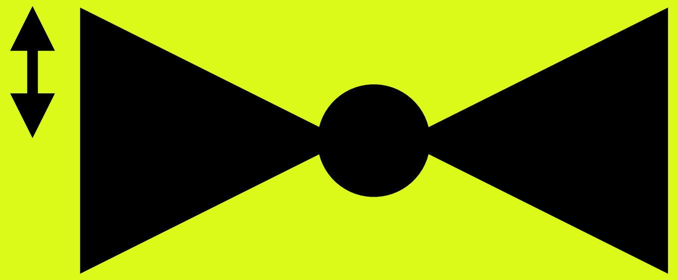

Scale Height H << Mean free path of Coulomb collision

-> **Collisionless system** in the RIAF

-> Electrons and protons cannot be the Maxwell distribution.

Particles can be the power-law distribution if the particles are accelerated.

Inefficient coulomb collision in the MAD

$$\boxed{\lambda_c \sim \frac{1}{n\sigma_c}}$$

$$n = \frac{\rho}{m_p},\ \rho \approx \frac{\dot{M}}{4\pi RHV_R}$$

$$\therefore n \simeq \frac{4c^2}{\sigma_T GM_\odot}\dot{m}m^{-1}r^{-3/2}\alpha^{-1}$$

$$\sigma_c \simeq \pi\left(\frac{e^2}{kT}\right),\ kT \sim m_e c^2$$ (ex. electron)

$$\therefore \frac{1}{n\sigma_c} = \frac{2}{3}\frac{GM_\odot}{c^2}\dot{m}^{-1}mr^{3/2}\alpha$$

On the other hand,

$$H \simeq \frac{1}{2}R = \frac{1}{2}\frac{GM_\odot}{c^2}mr$$

$$\therefore \frac{H}{\lambda_c} \sim 3\dot{m}r^{-1/2}\alpha^{-1}$$

$\dot{m} \ll 1,\ r \sim 10,\ \alpha \sim 0.3$ -> $H \ll \lambda_c$

Since the mean free path of the coulomb collision is much longer than the scale height of the accretion disk, the particle in the MADs are not thermalize.

The definition of the MAD

The magnetic flux connected to the horizon of the Black Hole: ϕ_{BH}

$$\phi_{\mathrm{BH}} = \frac{1}{2\sqrt{\dot{M}R_g c}} \int_\theta \int_\phi |B^r(r_{\mathrm{H}}, t)| \, dA_{\theta\phi}$$

The definition of the MAD state is that the $\phi_{\mathrm{BH}} \approx 50$ Narayan et al. (2012)

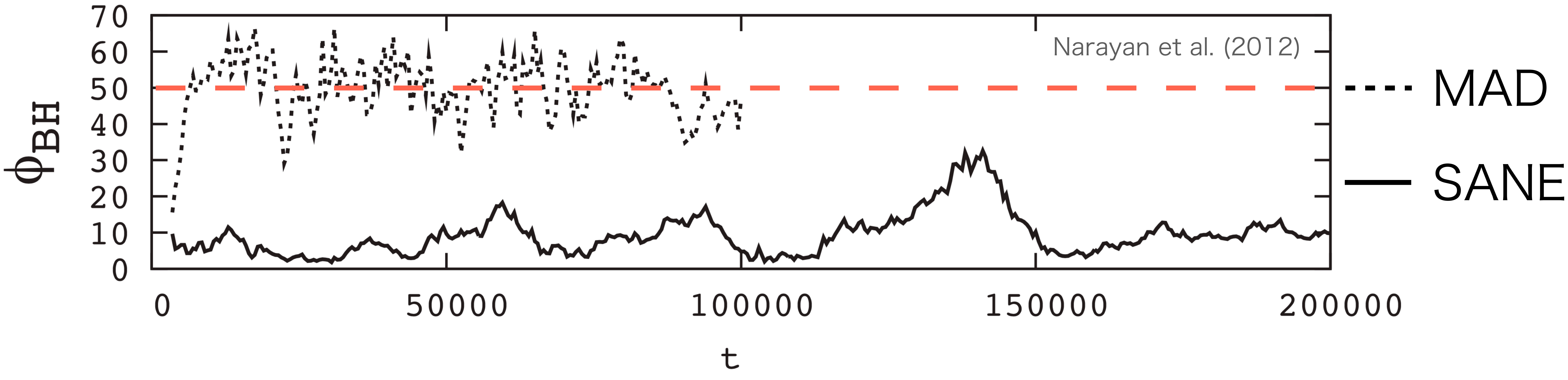

Estimate of the magnetic field

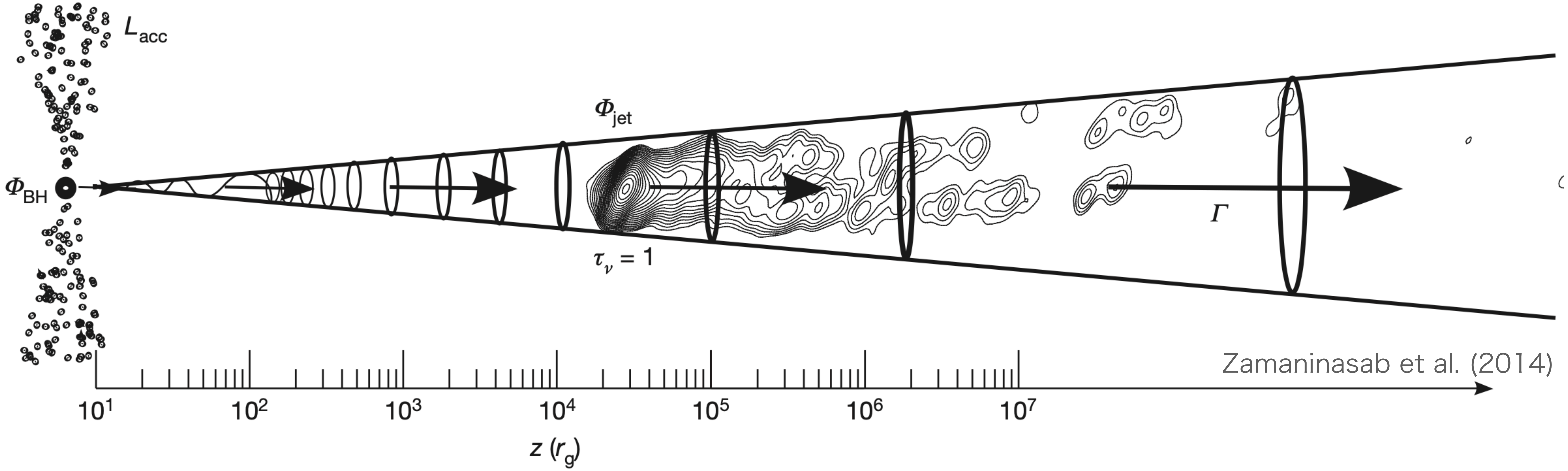

optical depth = $\alpha_j R \sim \frac{\epsilon_j}{B_\nu} R \propto \frac{n_e P_\nu R}{B_\nu}$、 $P_\nu \sim B\left(\frac{\nu}{B}\right)^{1/3}$ Optically thick by the Synchrotron-self absorption

By observation of other wavelength and comparing the size of the optically thick region, we can estimate the magnetic field.

↓

It is important that we have enough spatial resolution to estimate the optically thick region.

Magnetic Reconnection

Magnetic fields diffuse and dissipate due to the magnetic resistance

$$\frac{\partial B_y}{\partial t} = \eta \frac{\partial^2 B_y}{\partial x^2}$$

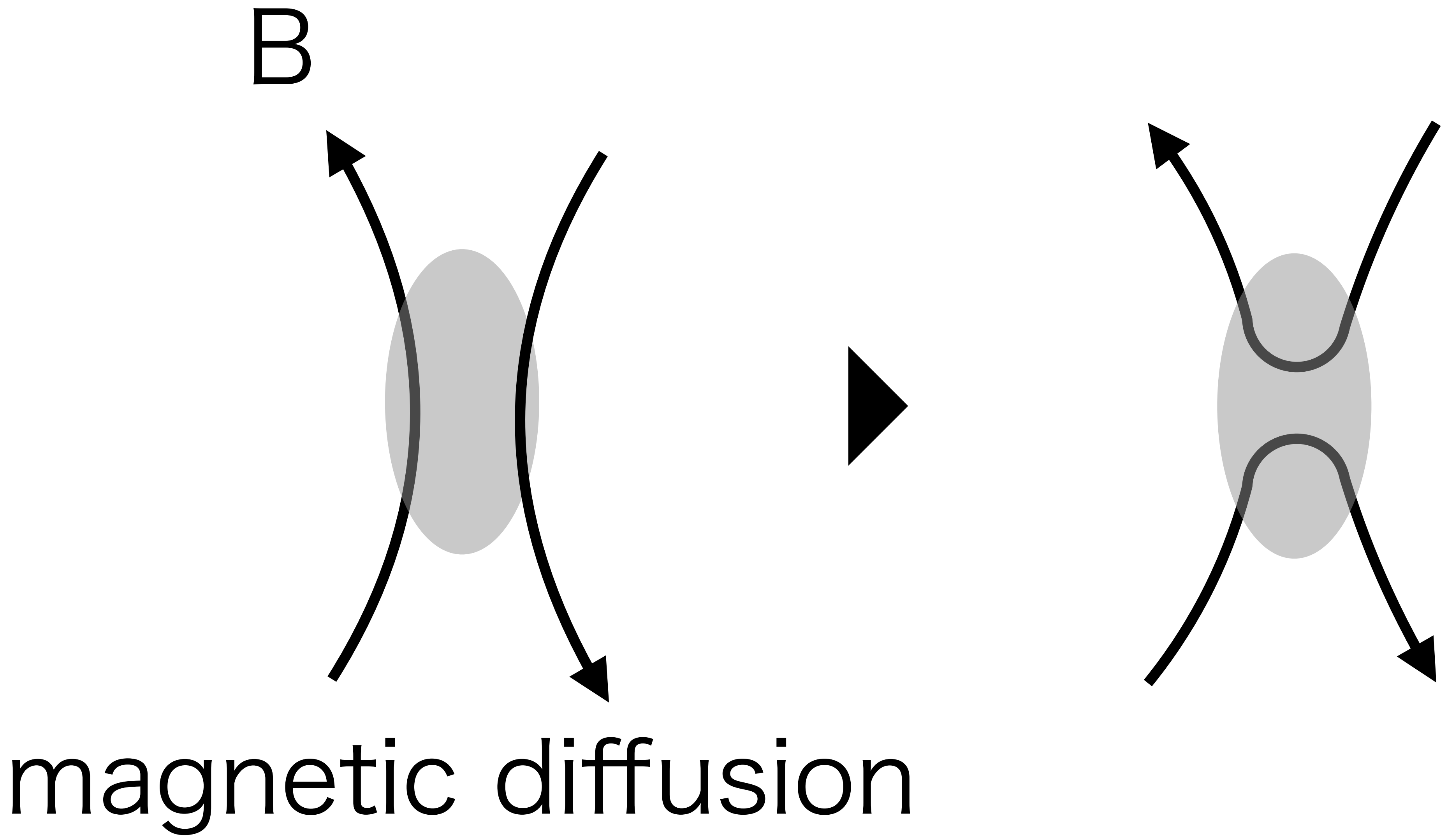

Particles are accelerated by

(i) E field at x-point

(ii) Back and forth between plasmoids

Similar to Fermi acceleration mechanism

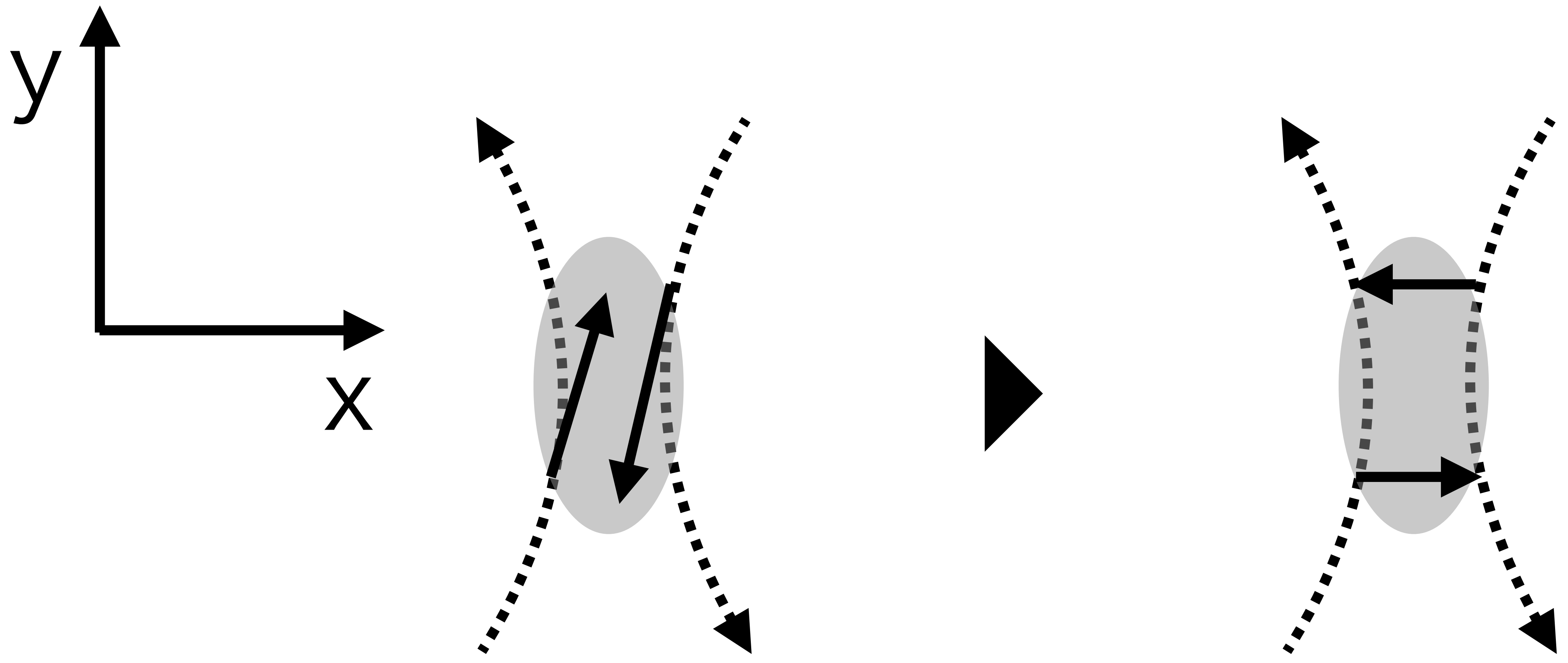

Problem of the hadronic jet model

Hadronic jet model

Gamma-rays are produced by the non-thermal proton synchrotron.

(i) Jet power higher than the Eddington luminosity is required.
-> It is opposed that the accretion rate is lower than the Eddington rate.

(ii) For M87, the jet is off-axis and the beaming factor should be small ($\delta \sim 2/(\Gamma\theta_v^2)$), but the required beaming factor is as high as $\delta \approx \Gamma$.

Parameters of the MAD model

Steady & one-zone approximation

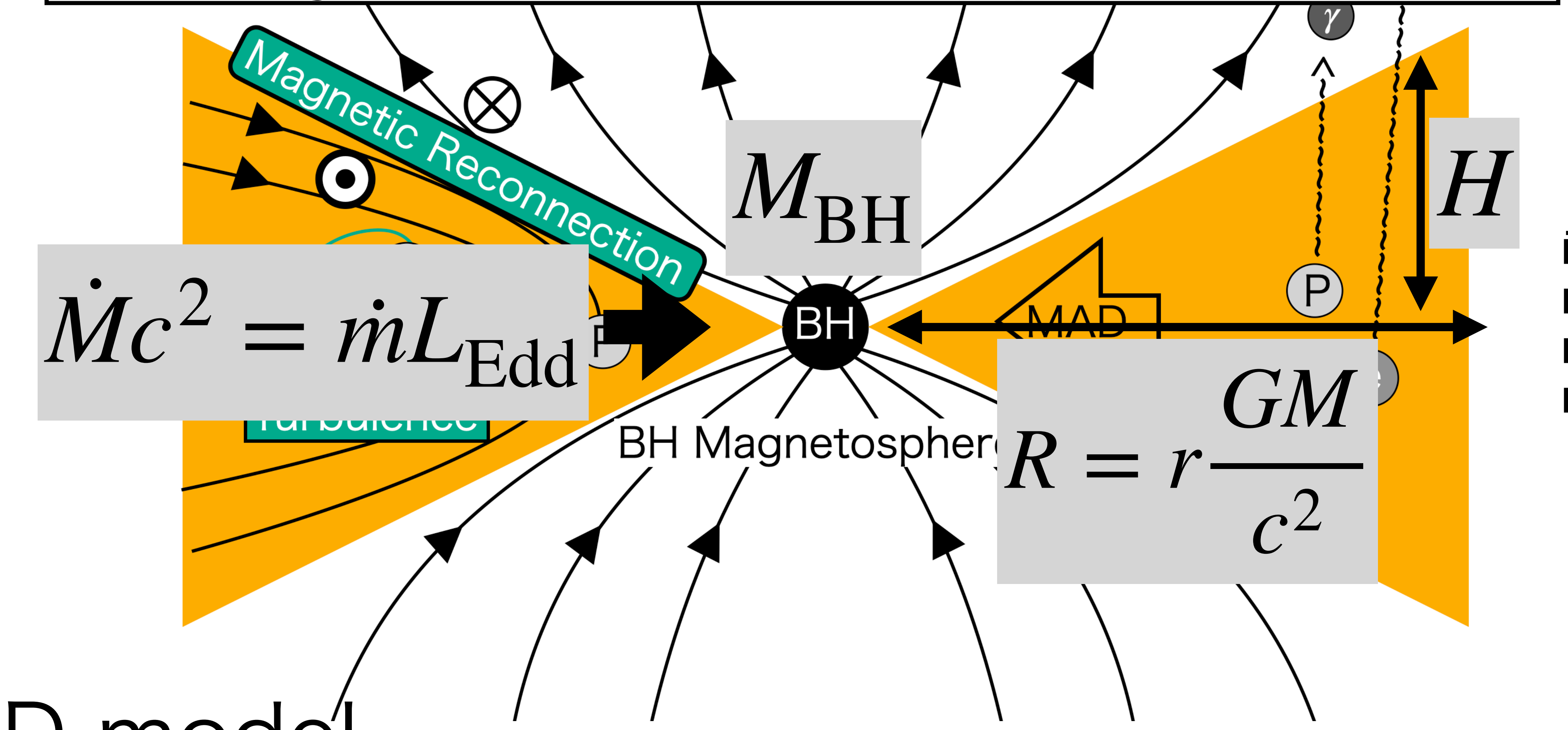

Steady and homogeneous flows are accreted onto the BH

Parameters of the MAD model

$M_{\rm BH} = m M_\odot$	$\dot{M}c^2 = \dot{m} L_{\rm Edd}$
$R = r\frac{GM}{c^2}$	Alpha viscosity: α
$\beta = \frac{P_{\rm gas}}{P_{\rm B}}$	$L_{\rm tot} = \epsilon_{\rm dis}\dot{M}c^2$ $L_{\rm non,thml} = \epsilon_{\rm NT}\epsilon_{\rm dis}\dot{M}c^2$
$l_{\rm mfp} = \eta\frac{E_i}{eB}$	Injection index: $s_{\rm inj}$

Quantities of the parameters are restricted by the physical requirement.
-> **MAD model cannot reproduce all of the SEDs.**

Mass density : $\rho \approx \frac{\dot{M}}{4\pi R H V_R} \propto \dot{m} m^{-1} r^{-3/2} \alpha^{-1}$

Magnetic field : $B = \sqrt{\frac{8\pi\rho C_s^2}{\beta}} \propto \dot{m}^{1/2} m^{-1/2} r^{-5/4} \alpha^{-1/2} \beta^{-1/2}$

Classification of the results

① Calculate the χ^2

$$\chi^2 = \sum_i \left(\frac{F_{\mathrm{data},i} - F_{\mathrm{model},i}}{\sigma_i} \right)^2$$

- $F_{\mathrm{data},i}$: Observational flux in the GeV band
- $F_{\mathrm{model},i}$: Calculated flux in the GeV band by the MAD model
- σ_i: Observational error

We evaluate the χ^2 by using the **GeV data.**

We consider that the photons in other bands are produced by the jet.

We calculate the χ^2 **by only changing the $\dot{m}$**

② Calculate and evaluate the Q

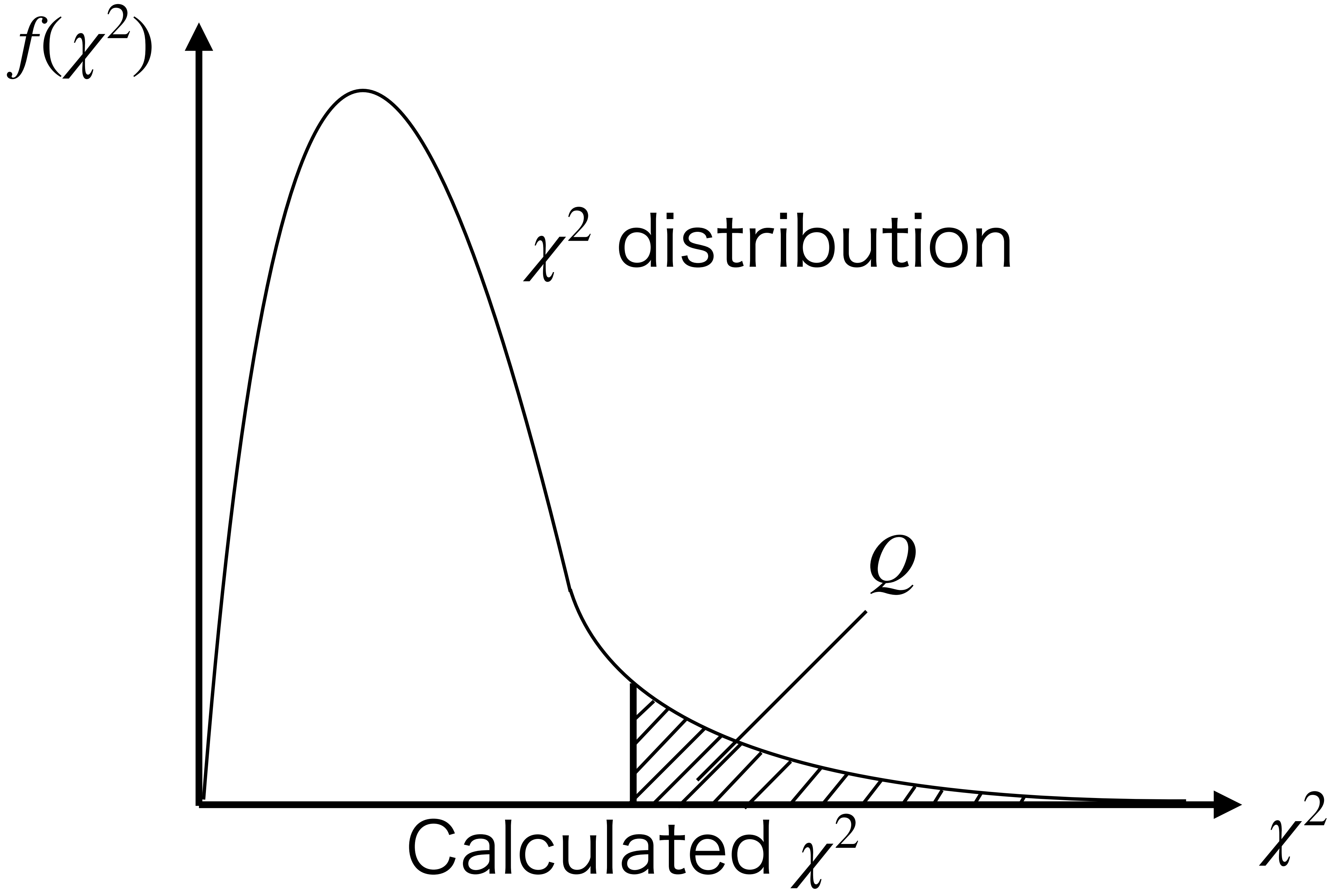

. $Q > 0.01$:

MAD model **can** reproduce the GeV data.

. $Q < 0.01$:

MAD model **cannot** reproduce the GeV data.

Gamma-ray luminosity to accretion rate

We plot the gamma-ray luminosity(Observational value) to accretion rate $[\mathrm{M_\odot\ yr^{-1}}]$(Calculated value).

For a higher $\dot{m}$
-> **Low** L_γ due to the absorption by the $\gamma\gamma$ interaction

For a lower $\dot{m}$
-> **Low** L_γ due to the inefficient radiation
(i.e., $t_{\mathrm{diff}} < t_{\mathrm{syn}}$)

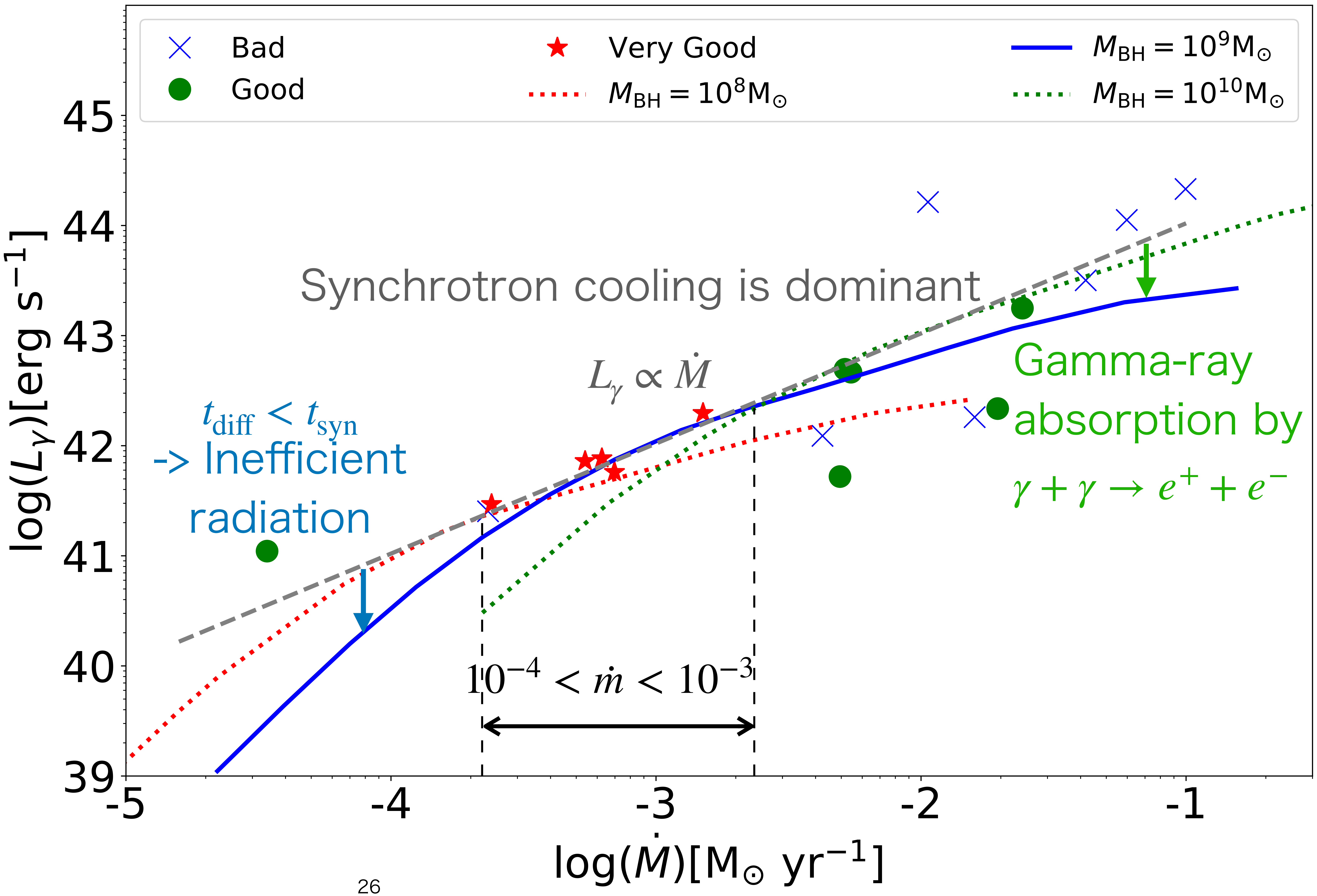

Calculation Method (Thermal)

Parameter set: $M_{\rm BH} = mM_\odot,\ \dot{M}c^2 = \dot{m}L_{\rm Edd},\ R = r\frac{GM}{c^2},\ \alpha,\ \beta,\ \epsilon_{\rm NT},\ \epsilon_{\rm dis},\ \eta,\ s_{\rm inj}$

$L_{\rm tot} = \epsilon_{\rm dis}\dot{M}c^2$

$L_{\rm non,thml} = \epsilon_{\rm NT}\epsilon_{\rm dis}\dot{M}c^2$

Thermal electron component

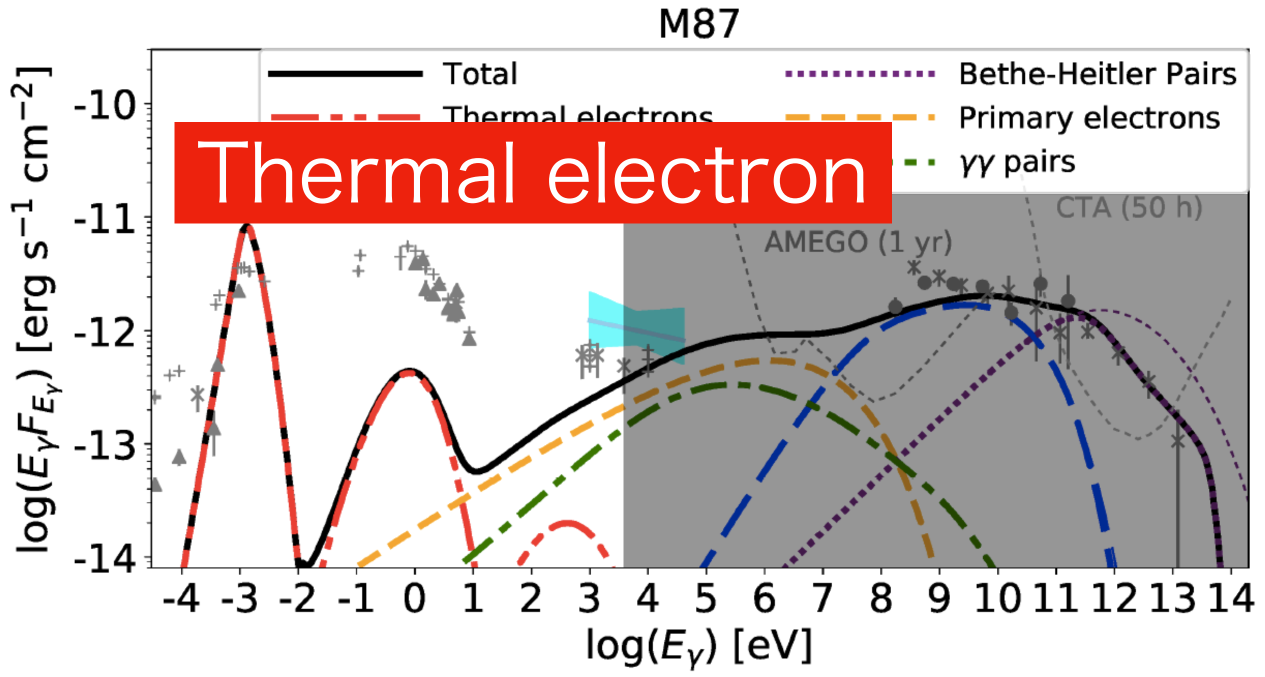

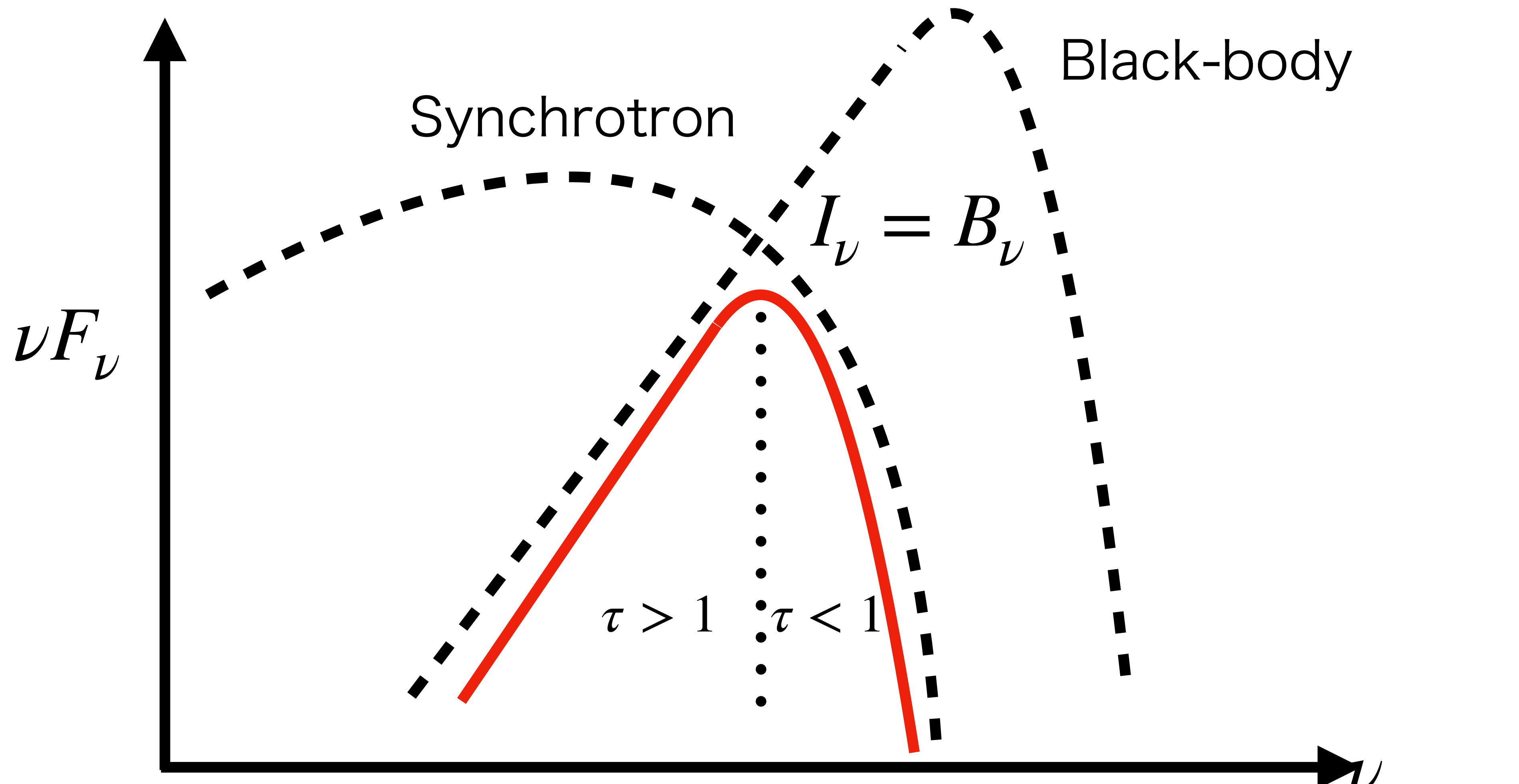

- Radiation process

  Synchrotron + Inverse Compton (IC) (+Bremsstrahlung)

- Electron heating rate: $\frac{\mathcal{Q}_e}{\mathcal{Q}_p} = \left(\frac{m_e T_e}{m_p T_p}\right)^{1/4}$ Hoshino 2018

$\tau > 1$: Optically thick by the synchrotron-self absorption and Black-body radiation.

$\tau < 1$: Synchrotron radiation by the thermal electron

- By solving $L_{\nu,\rm thml} \approx \left(\frac{\mathcal{Q}_e}{\mathcal{Q}_p}\right)(1-\epsilon_{\rm NT})\,\epsilon_{\rm dis}\dot{m}L_{\rm Edd}$ for the temperature

  -> Calculate photon spectra

Calculate iteratively

$$L_{\nu,\rm thml} \sim 16\sqrt{2\pi}\frac{m_p^{\frac{3}{2}}G^{\frac{1}{2}}M_\odot^{\frac{1}{2}}k_B^{\,5}e^3}{\sigma_T^{\frac{3}{2}}m_e^{\,9}c^{15}}T_e^{\,7}\dot{m}^{\frac{3}{2}}m^{\frac{1}{2}}r^{-\frac{7}{4}}\alpha^{-\frac{3}{2}}\beta^{-\frac{3}{2}}$$

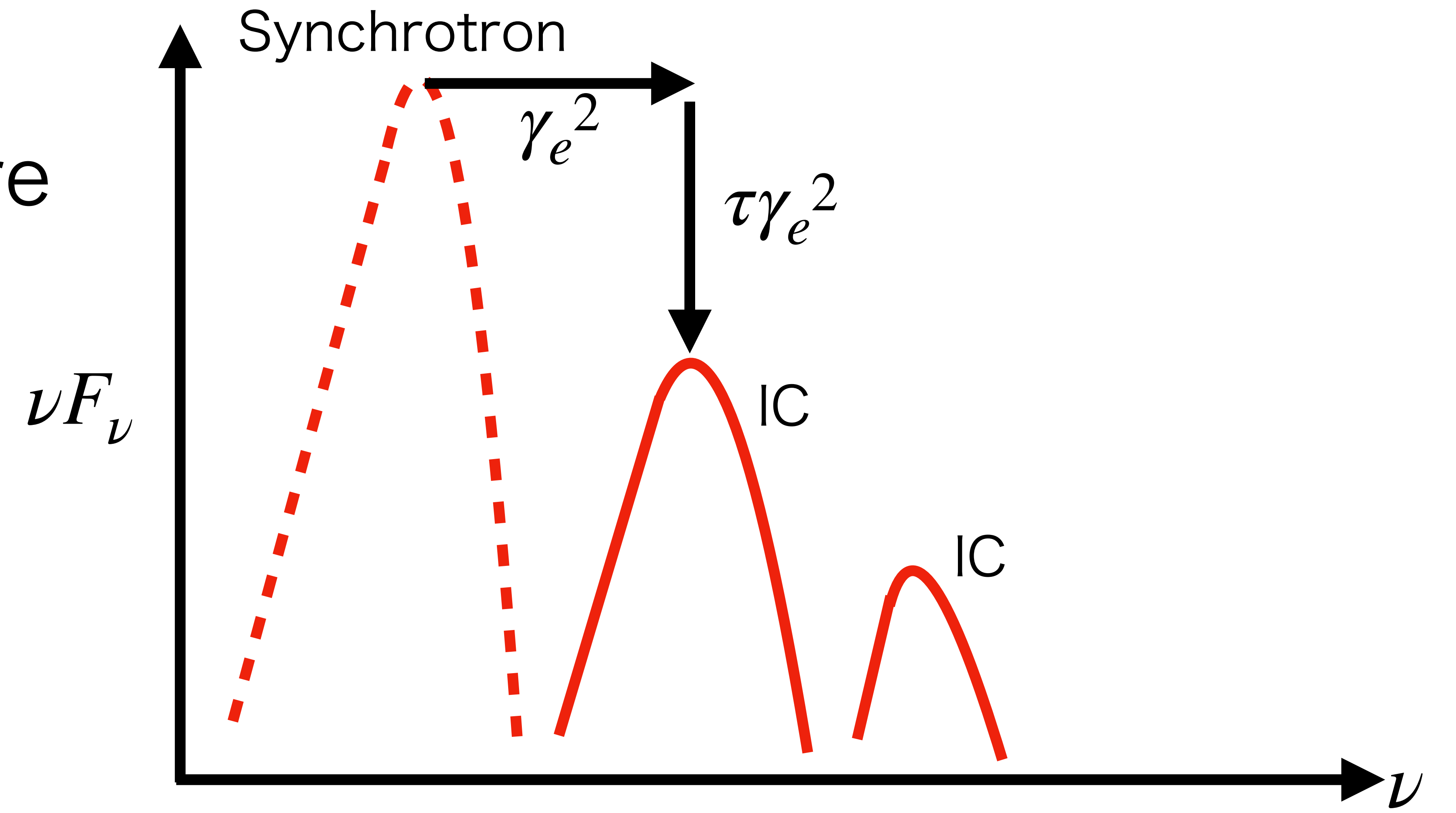

The peak luminosity of the thermal synchrotron

$Q_{\rm tot} = \epsilon_{\rm dis}\dot{M}c^2$

$Q_{\rm non,thml} = \epsilon_{\rm NT}\epsilon_{\rm dis}\dot{M}c^2$

Parameter set: $M_{\rm BH} = mM_\odot,\ \dot{M}c^2 = \dot{m}L_{\rm Edd},\ R = r\frac{GM}{c^2},\ \alpha,\ \beta,\ \epsilon_{\rm NT},\ \epsilon_{\rm dis},\ \eta,\ s_{\rm inj}$

1. We obtain the ν_c by $I_\nu = B_\nu$.

-> $\nu_c = \frac{eB}{2\pi m_e c}\left(\frac{k_B T_e}{m_e c^2}\right)^2 x_M \quad (x_M : \text{const})$

2. Rayleigh-Jeans regime at the peak frequency.

-> $L_{\nu_c} \approx 4\pi R^2 \times 2\pi \frac{{\nu_c}^2}{c^2} k_B T_e$

B_ν

3. We obtain the $L_{\nu,\rm thml}$ by $L_{\nu,\rm thml} \approx \nu_c L_{\nu_c}$.

-> $L_{\nu,\rm thml} = 16\sqrt{2\pi}\frac{{m_p}^{\frac{3}{2}} G^{\frac{1}{2}} {M_\odot}^{\frac{1}{2}} {k_B}^5 e^3}{{\sigma_T}^{\frac{3}{2}} {m_e}^9 c^{15}} {T_e}^7 \dot{m}^{\frac{3}{2}} m^{\frac{1}{2}} r^{-\frac{7}{4}} \alpha^{-\frac{3}{2}} \beta^{-\frac{3}{2}} {x_M}^3$

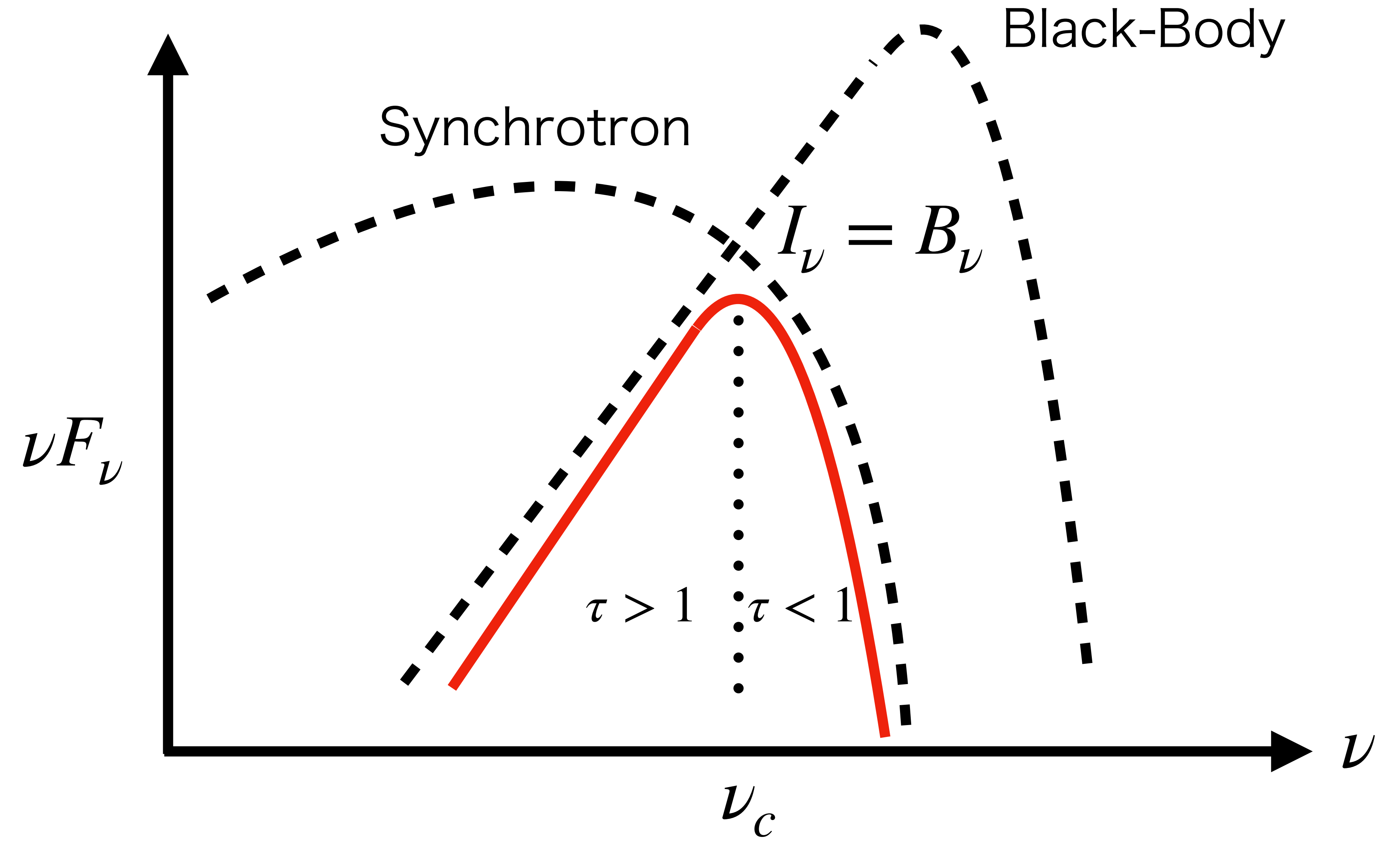

Equation of Continuity

Parametr set: $M_{\rm BH} \underset{\rm M87}{=} mM_\odot,\ \dot{M}c^2 = \dot{m}L_{\rm Edd},\ R = r\frac{GM}{c^2},\ \alpha,\ \beta,\ \epsilon_{\rm NT},\ \epsilon_{\rm dis},\ \eta,\ s_{\rm inj}$

$Q_{\rm tot} = \epsilon_{\rm dis}\dot{M}c^2$

$Q_{\rm non,thml} = \epsilon_{\rm NT}\epsilon_{\rm dis}\dot{M}c^2$

Non-thermal component

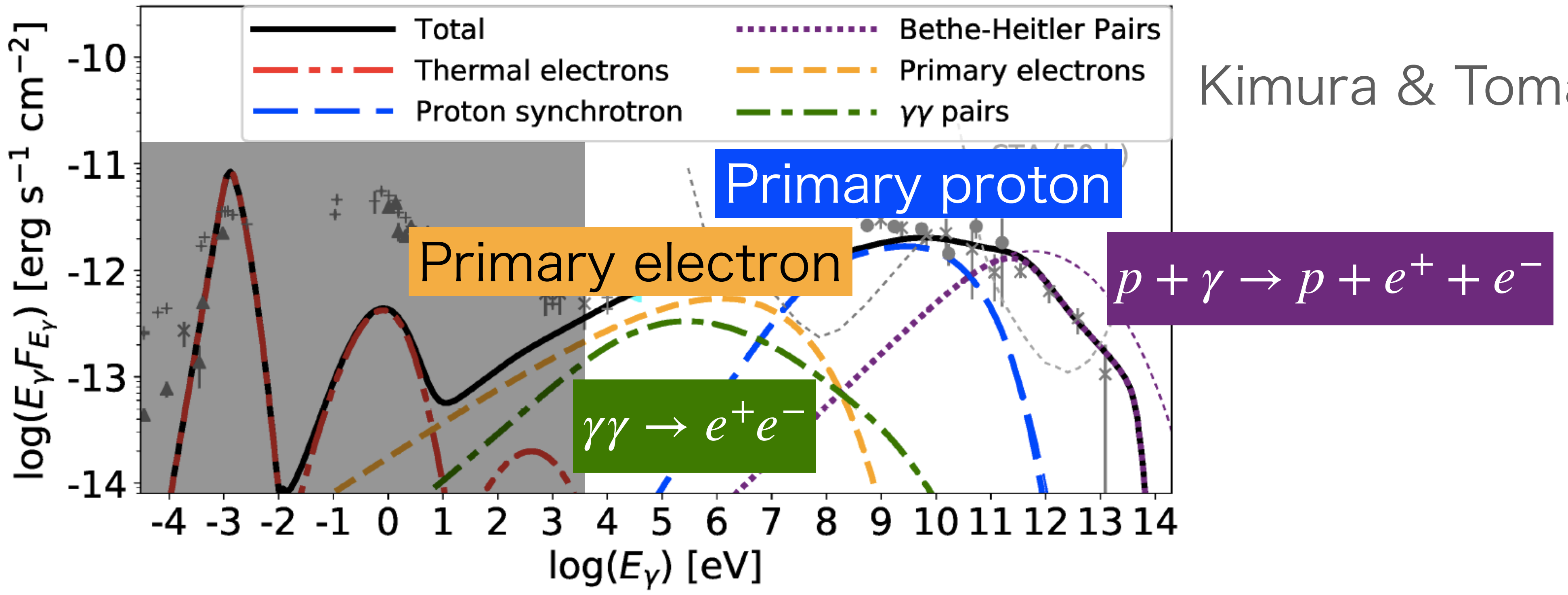

Kimura & Toma 2020

■ Transport equation in energy space

$$\frac{\partial N_{E_i}}{\partial t} = \dot{N}_{E_{i,\rm inj}} + \nabla\cdot\left(D_{xx}\nabla N_{E_i} - \boldsymbol{v}N_{E_i}\right) + \frac{\partial}{\partial E_i}\left(\frac{E_i}{t_{i,\rm cool}}N_{E_i} + E_i^2 D_{E_i}\frac{\partial}{\partial E_i}\left(\frac{N_{E_i}}{E_i^2}\right)\right)$$

Injection | Diffusion | Advection | Cooling | Momentum Diffusion (Acceleration by the turbulence)

Steady & one-zone

$$-\frac{d}{dE_i}\left(\frac{N_{E_i}E_i}{t_{i,\rm cool}}\right) = \dot{N}_{E_i,\rm inj} - \frac{N_{E_i}}{t_{\rm esc}}$$

Cooling | Injection | Escape

$$\dot{N}_{E_{i,\rm inj}} \approx \dot{N}_0\left(\frac{E_i}{E_{i,\rm cut}}\right)^{-s_{\rm inj}}\exp\left(-\frac{E_i}{E_{i,\rm cut}}\right)$$

■ Cooling time $t_{i,\rm cool}$

(i) Synchrotron cooling

(ii) Proton-photon interaction

(iii) pp collision

■ Escape time $t_{\rm esc}$

(i)Infall

(ii)Diffusion

Calculation Method (Non-thermal)

$Q_{\rm tot} = \epsilon_{\rm dis}\dot{M}c^2$

Parametr set: $M_{\rm BH} \underset{\rm M87}{=} mM_{\odot}$, $\dot{M}c^2 = \dot{m}L_{\rm Edd}$, $R = r\frac{GM}{c^2}$, α, β, $\epsilon_{\rm NT}$, $\epsilon_{\rm dis}$, η, $s_{\rm inj}$ $Q_{\rm non,thml} = \epsilon_{\rm NT}\epsilon_{\rm dis}\dot{M}c^2$

Non-thermal component

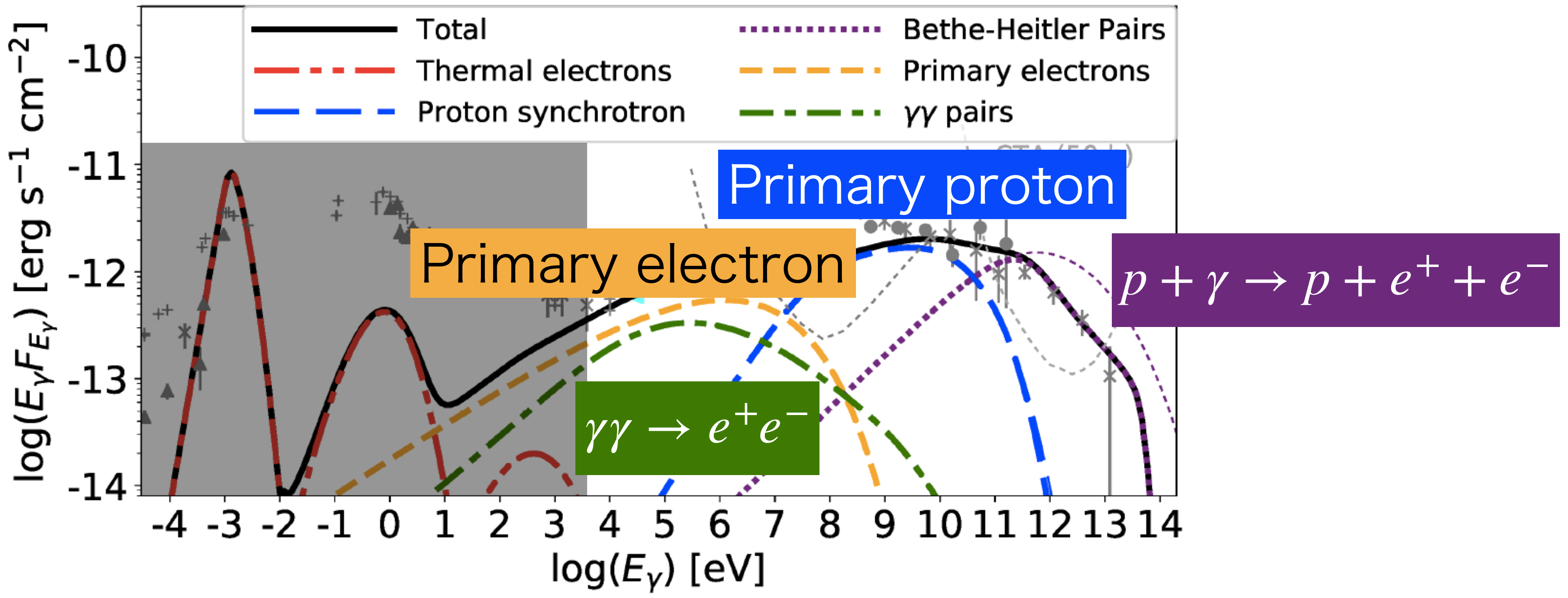

Kimura & Toma 2020

Transport eq. $-\frac{d}{dE_i}\left(\frac{N_{E_i}E_i}{t_{i,\rm cool}}\right) = \dot{N}_{E_i,\rm inj} - \frac{N_{E_i}}{t_{\rm esc}}$

$$\dot{N}_{E_{i,\rm inj}} \approx \dot{N}_0 \left(\frac{E_i}{E_{i,\rm cut}}\right)^{-s_{\rm inj}} \exp\left(-\frac{E_i}{E_{i,\rm cut}}\right)$$

- $L_e \approx \int \dot{N}_{E_{e,\rm inj}} E_e dE_e \approx \left(\frac{\mathcal{Q}_e}{\mathcal{Q}_p}\right)\epsilon_{\rm NT}\epsilon_{\rm dis}\dot{M}c^2$ & Transport eq.
- $L_p \approx \int \dot{N}_{E_{p,\rm inj}} E_p dE_p \approx \epsilon_{\rm NT}\epsilon_{\rm dis}\dot{M}c^2$ & Transport eq.

① Calculate the number spectrum of the non-thermal particle -> Calculate the photon spectrum.

- ② By using the number spectrum of non-thermal protons and the photon spectra, we calculate the number spectrum of secondary electron-positron pairs by the Bethe-Heitler process ($p+\gamma \to p+e^+ + e^-$). -> We calculate the photon spectrum.
- ③ By using the total photon spectra, we calculate the number spectrum of secondary electron-positron pairs by the two-photon interaction ($\gamma+\gamma \to e^+ + e^-$) -> We calculate the photon spectrum.

Calculate iteratively

Radio galaxies and MADs

Magnetic flux of the jet Φ_{jet}(Observation, vertical axis)

v.s.

$L_{acc}^{1/2}M_{acc}$(Correlate to the magnetic flux in the MAD scenario, horizontal axis)

Dash line:
Theoretical prediction
based on the MAD model.

Applying the 76
Radio-loud AGNs

$\phi \sim 50\sqrt{\dot{M}r_g c} \propto L_{acc}^{1/2}M$ (for MAD)

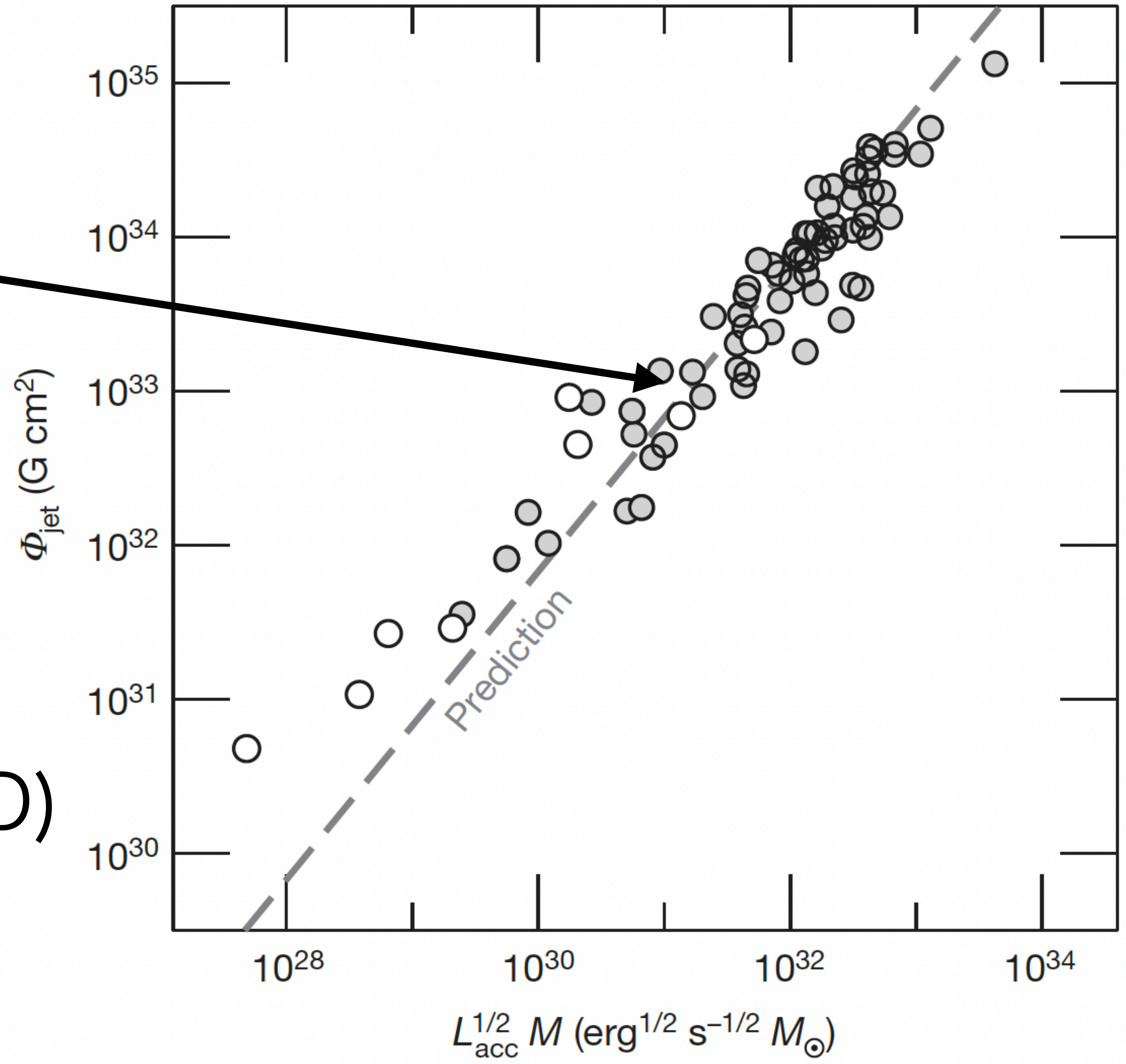

Gray filled circle : Blazars
White circle : Radio galaxies

Figure 2 | Measured magnetic flux of the jet, Φ_{jet}, versus $L_{acc}^{1/2}M$. Here we assume that $\Gamma\theta_j = 1$; we also assume an accretion radiative efficiency of $\eta = 0.4$ for our sample of 76 sources. The dashed line shows the theoretical prediction based on the magnetically arrested disk model.[31] Filled and open circles represent blazars and radio galaxies, respectively (see Methods for details).

Dependence of peak luminosity

Parameter set:

$\dot{m} = 10^{-4}, m = 10^{9}, r = 10, \alpha = 0.3, \beta = 0.1, \epsilon_{\rm NT} = 0.33, \epsilon_{\rm dis} = 0.15, \eta = 5, s_{\rm inj} = 1.3$

$$L_{E_{p,\rm cut}} \propto \dot{m}^{5/2} m^{3/2} r^{-7/4} \alpha^{-3/2} \beta^{-3/2} \epsilon_{\rm NT} \epsilon_{\rm dis}$$

$$L_{E_{e,\rm cut}} \propto T_{\rm e}^{1/4} \dot{m} m r^{1/4} \epsilon_{\rm NT} \epsilon_{\rm dis}$$

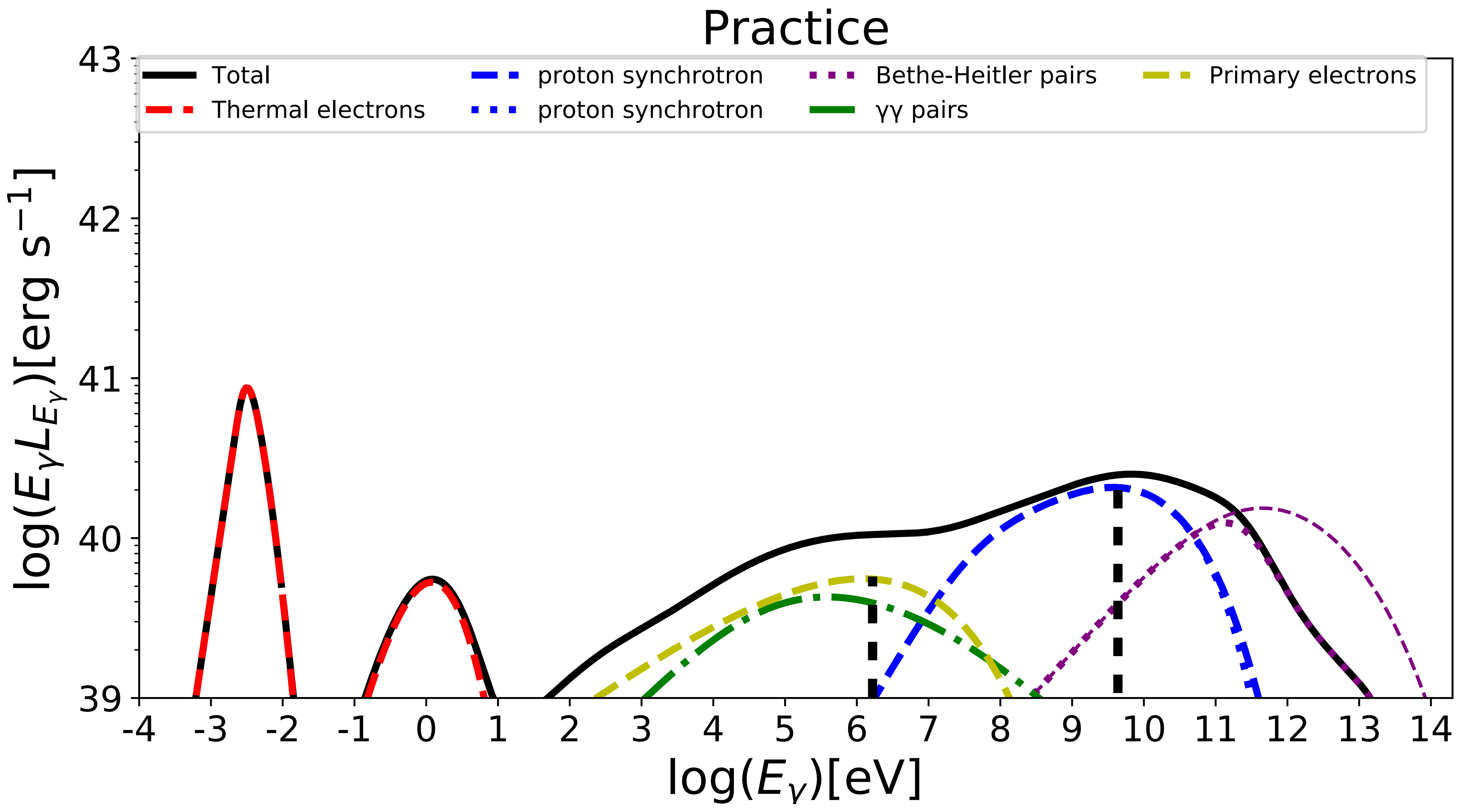

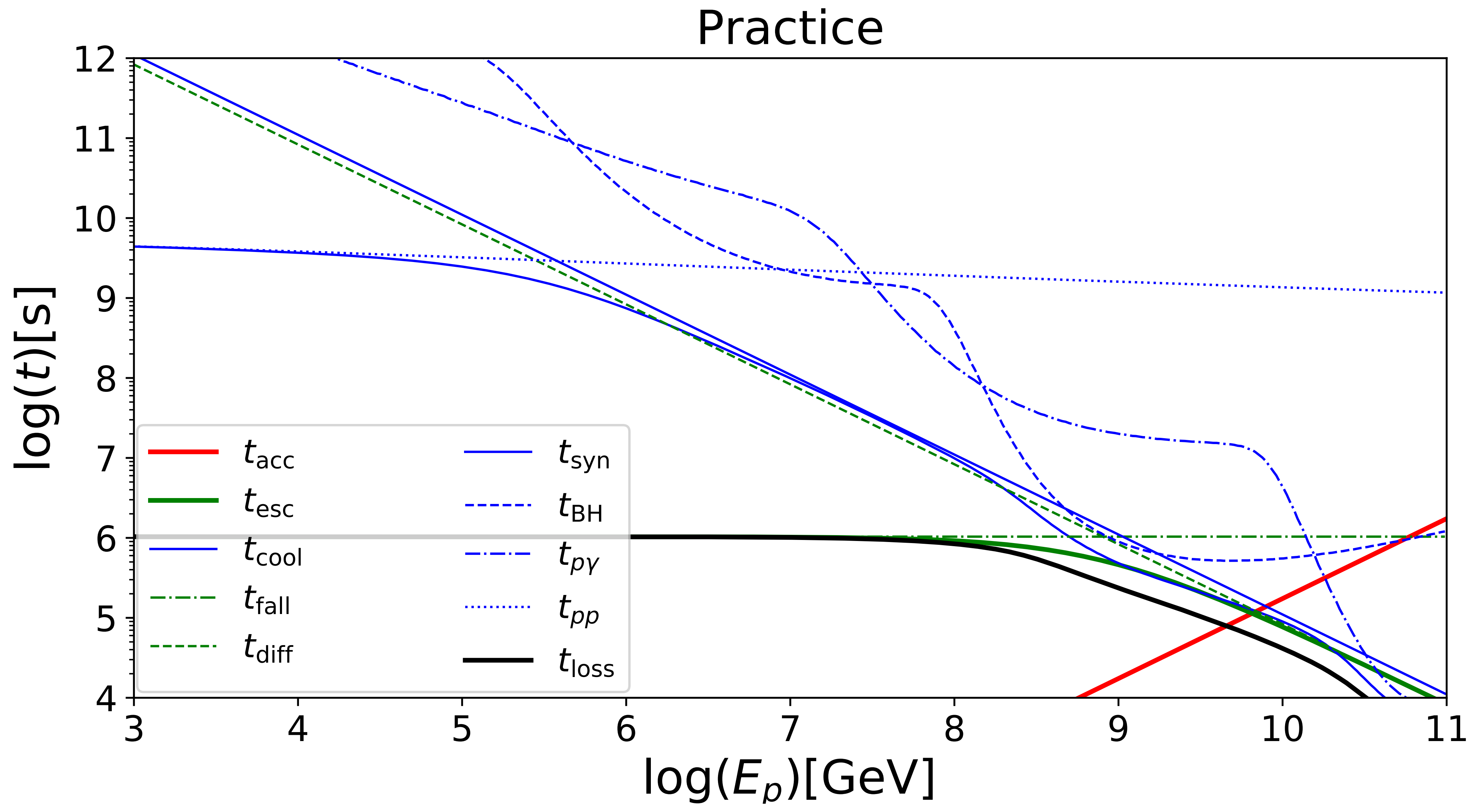

Physical parameter range

$\dot{m}$: **We allow the accretion rate as large as 10% of the Eddington rate.** If the accretion rate is larger than the 10% of Eddington rate, proton cooling by the coulomb collision is efficient, and thus, the accretion disk cannot be collisionless system. This critical accretion rate is determined by the proton heating rate is equal to the proton cooling rate by the coulomb collision. Cooling rate by the coulomb collision is proportional to the squared accretion rate.

r : $L = \epsilon_{\rm dis}\dot{M}c^2 = \frac{GM\dot{M}}{2R}$ is estimated by $\Delta E = -\frac{GMm}{R} + \frac{1}{2}mV_K{}^2$. The radio galaxies have relativistic jet, and thus, we consider that the central BH spins. Since the matter can exist outside of the innermost stable circular orbit, $\epsilon_{\rm dis}$ can be as large as 0.5 for the BH spin parameter a = 1. We consider that $\epsilon_{\rm dis}$~0.15, emission region r should be smaller than the 30.

$\epsilon_{\rm NT}$: This value is must be smaller than the 0.5 to sustain the structure of the accretion disk (Kimura et al. 2014).

α : We set α~0.3 because of the efficient angular momentum transport owing to the strong magnetic field in a MAD. (Narayan et al. 2012)

β : Because of the strong magnetic field, we take the value of β as 0.1 (there is no GRMHD simulation for β<<1). We note that if the value of β is much lower than 0.1, Alfven speed can be faster than the speed of light and the magnetic field can be much larger than the observed value. In the MHD simulation, the value of β is 0.1 at the edge of the accretion disk (White 2019).

Truncation radius of the accretion disk

Truncation radius is determined by the timescale

-> $t_{pe} = t_{\rm fall}$

For a high accretion rate, the truncation radius may be formed around 100-1000Rg, but the critical accretion rate by which the accretion disk is MAD is unknown.

Typically, the radius of the accretion disk of AGN is 1000AU, and thus, we consider that the emission region is not larger than the 1000AU.

Innermost region of accretion disks

At the transsonic point ($3r_s = 6r_g$), gas pressure (internal energy) decrease.

-> This is because the conversion of gravitational energy to the kinetic energy is more efficient than the conversion of that to the thermal energy.

-> Radial velocity increase, and the surface density decrease.

-> We consider that the transsonic point ($3r_s = 6r_g$) is the innermost radius of the accretion disk.

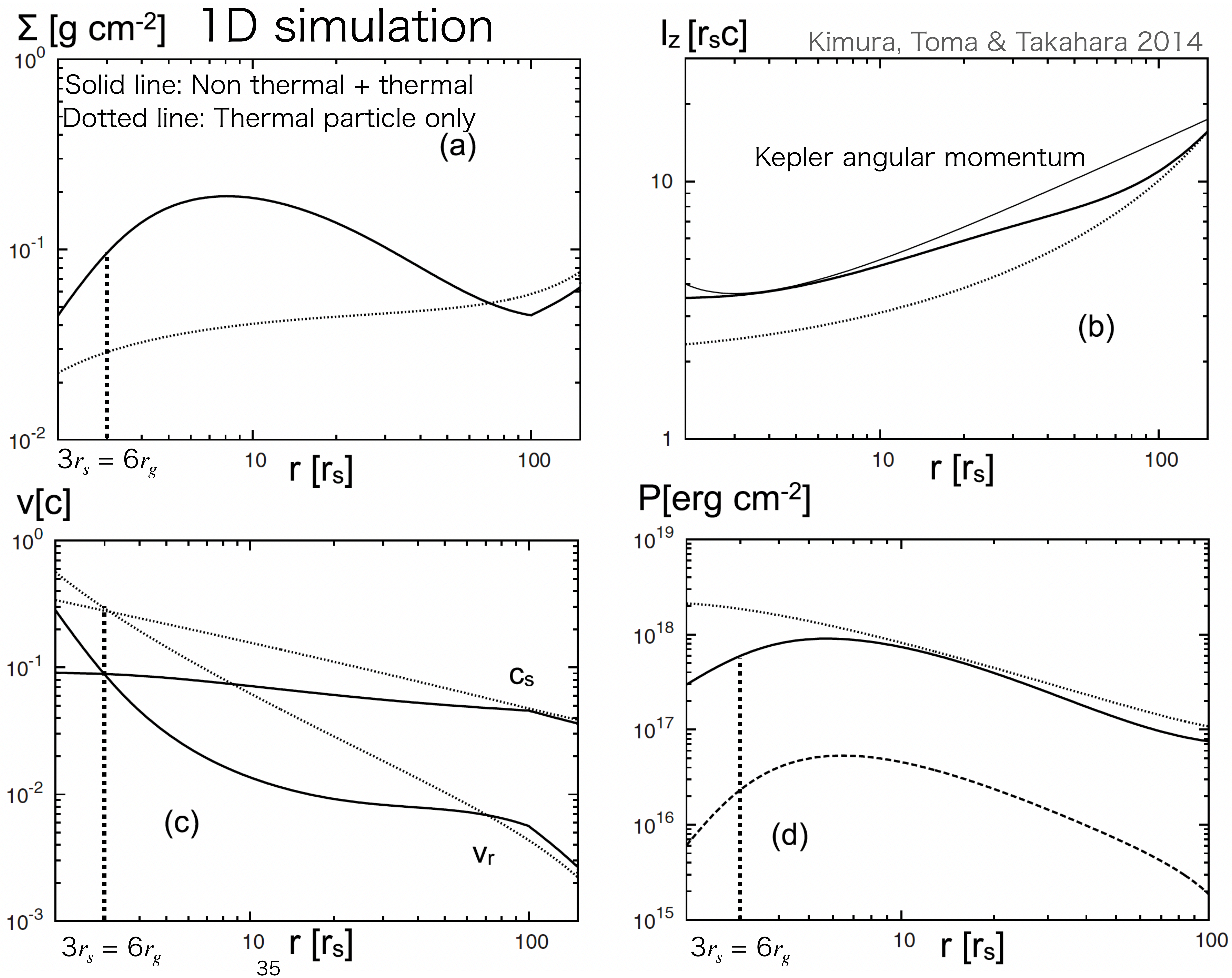

Sgr A*

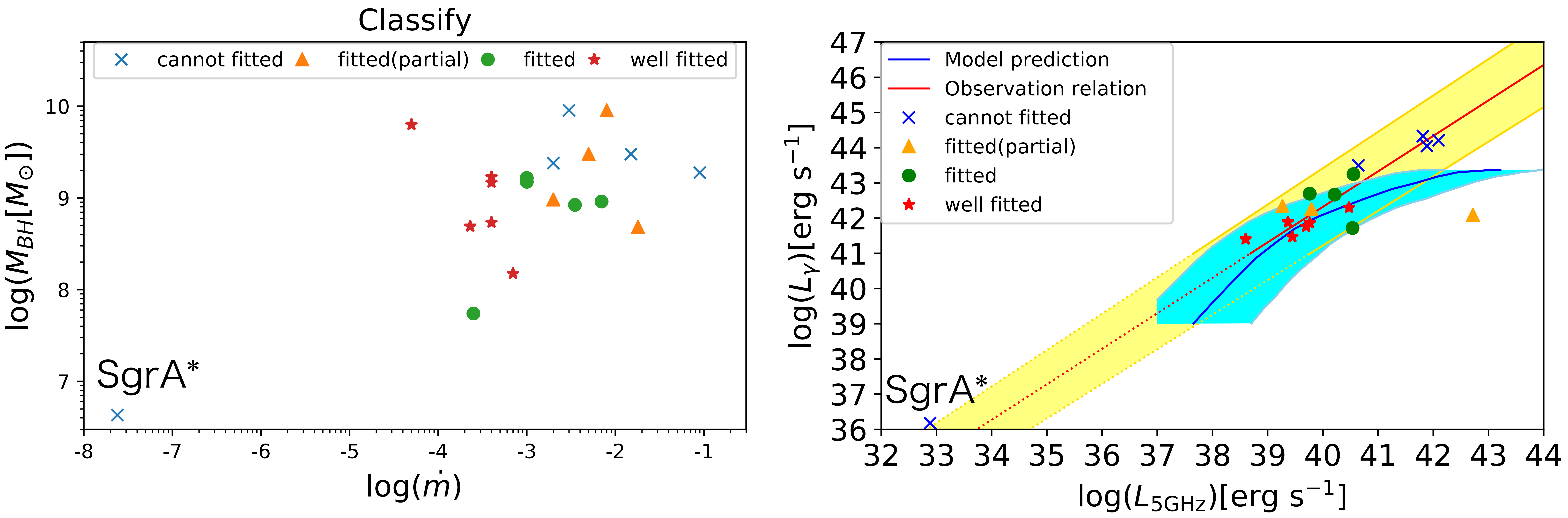

Sgr A* may not have a MAD.

Observational data of radio galaxies

Blue circle● :
LERG ($\dot{m}$ is lower than the 1% of the Eddington rate)

Green triangle▲ :
HERG ($\dot{m}$ is 1-10% of the Eddington rate)

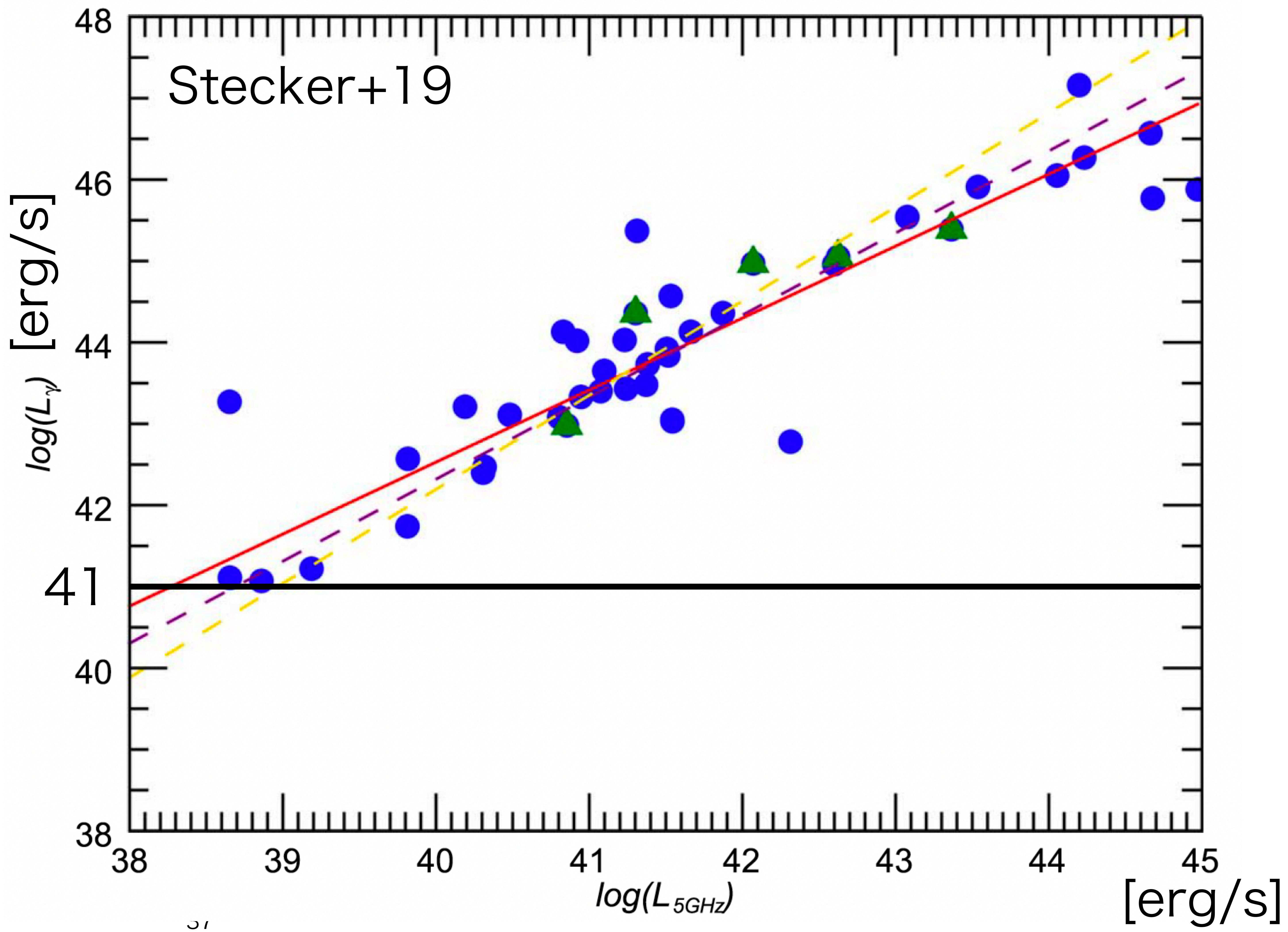

Each timescales

$$t_{syn} = \frac{E}{P_{syn}} \propto E^{-1} m \dot{m}^{-1}$$

$$t_{diff} = \frac{R^2}{D_R} \propto E^{-1} m^{\frac{3}{2}} \dot{m}^{\frac{1}{2}}$$

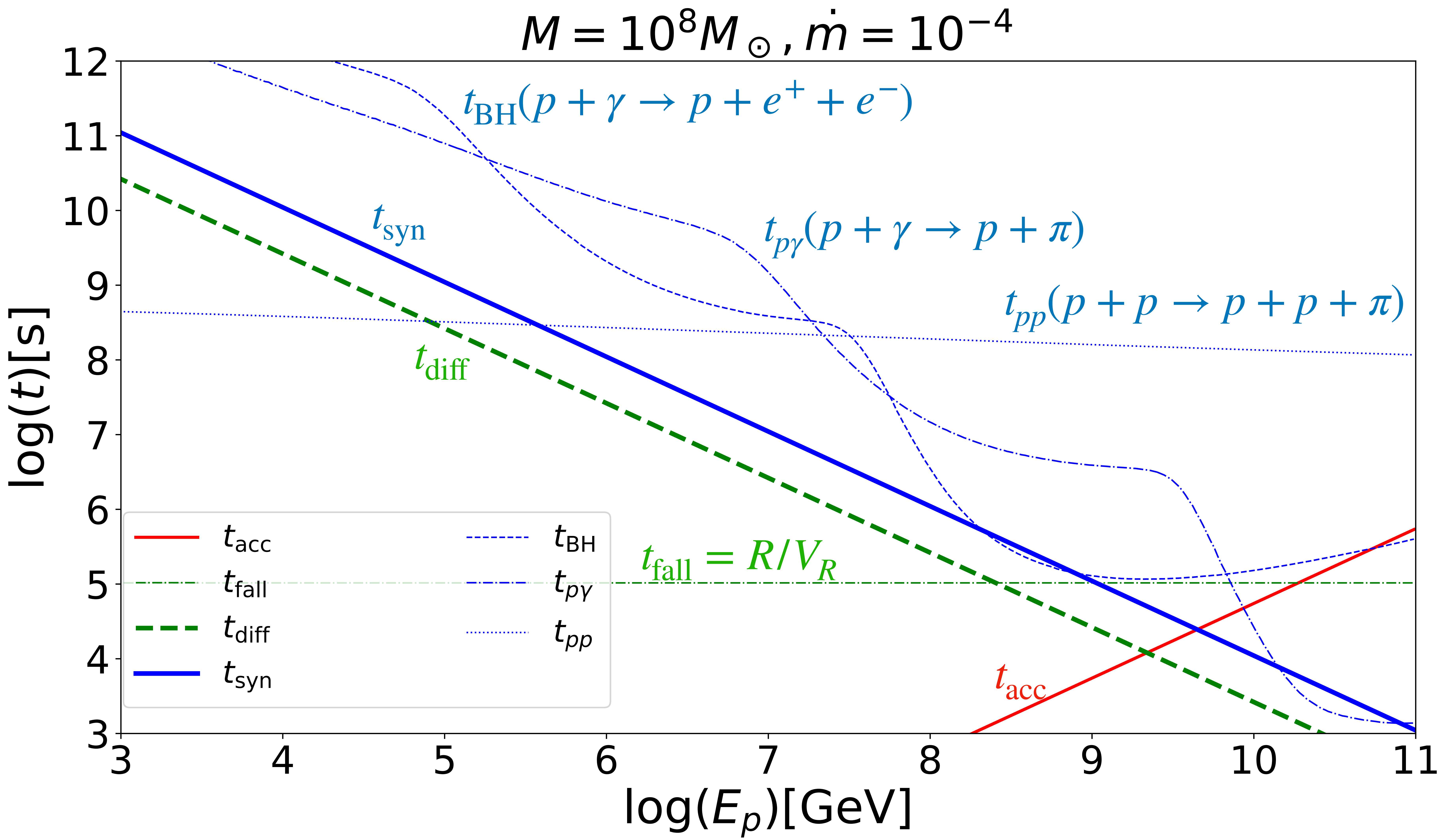

Each timescales

$$\frac{1}{t_{\rm loss}} = \frac{1}{t_{\rm esc}} + \frac{1}{t_{\rm cool}}$$

$$\frac{1}{t_{\rm esc}} = \frac{1}{t_{\rm fall}} + \frac{1}{t_{\rm diff}}$$

$$\frac{1}{t_{\rm cool,p}} = \frac{1}{t_{\rm syn}} + \frac{1}{t_{pp}} + \frac{1}{t_{p\gamma}} + \frac{1}{t_{\rm BH}}$$

$$\frac{1}{t_{\rm cool,e}} = \frac{1}{t_{\rm syn}}$$

$$t_{\rm acc} \propto E m^{\frac{1}{2}} \dot{m}^{-\frac{1}{2}}$$

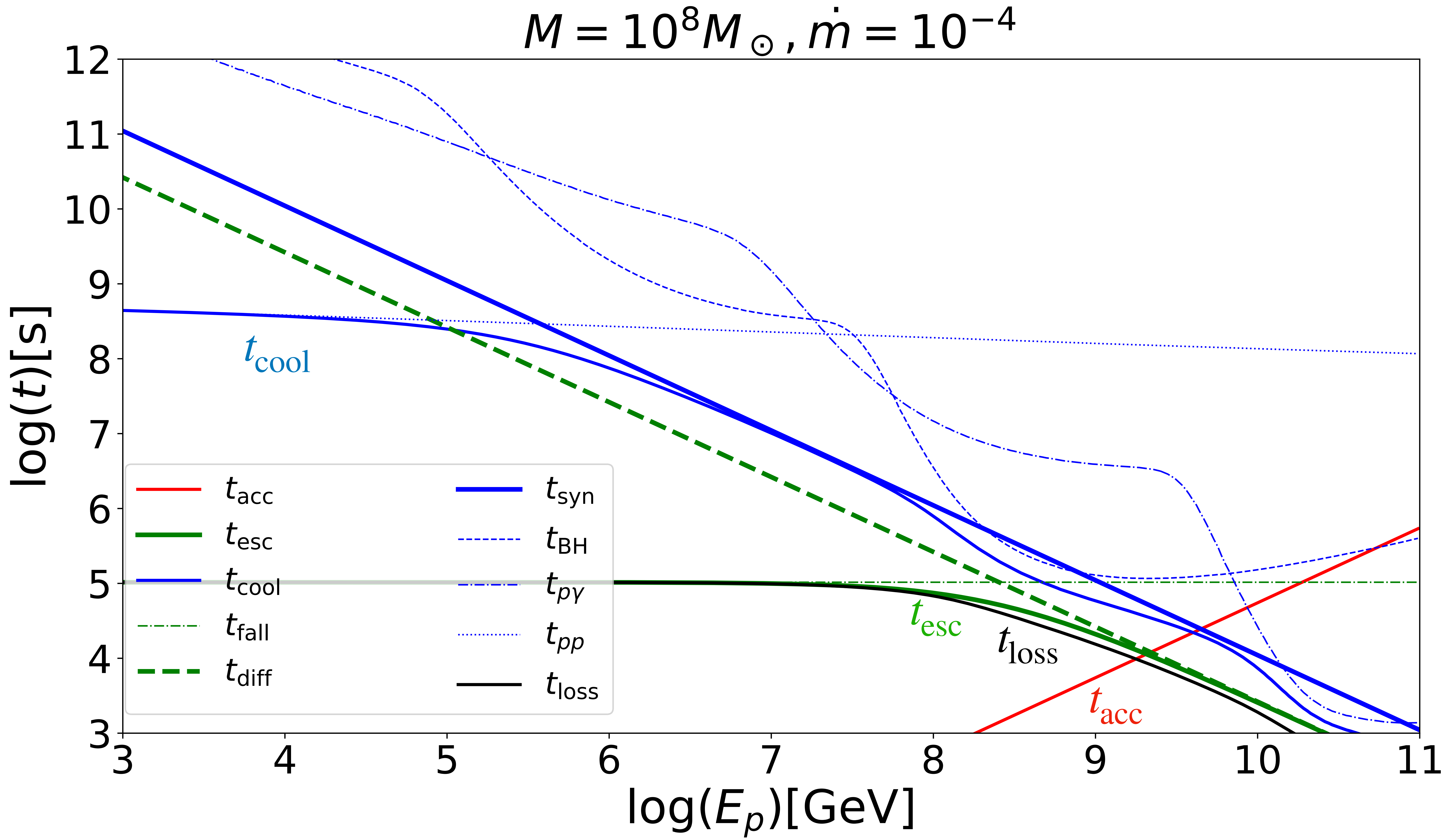

MAD model

Steady & one-zone approximation (Homogeneous emission region)

- Non-thermal component

Synchrotron radiation

$$L_{\mathrm{syn}} = \int N_{E_i} \cdot P_{\mathrm{syn}}\, dE_i \qquad N_{E_i} = \frac{dN}{dE_i}$$

- Equation of continuity in the energy space

$$-\frac{d}{dE_i}\left(\frac{N_{E_i}E_i}{t_{i,\mathrm{cool}}}\right) = \dot{N}_{E_i,\mathrm{inj}} - \frac{N_{E_i}}{t_{\mathrm{esc}}}$$

Cooling Injection Escape

■ Cooling time $t_{i,\mathrm{cool}}$ ■ Escape time t_{esc}

Schematic image of the equation of continuity in the energy space

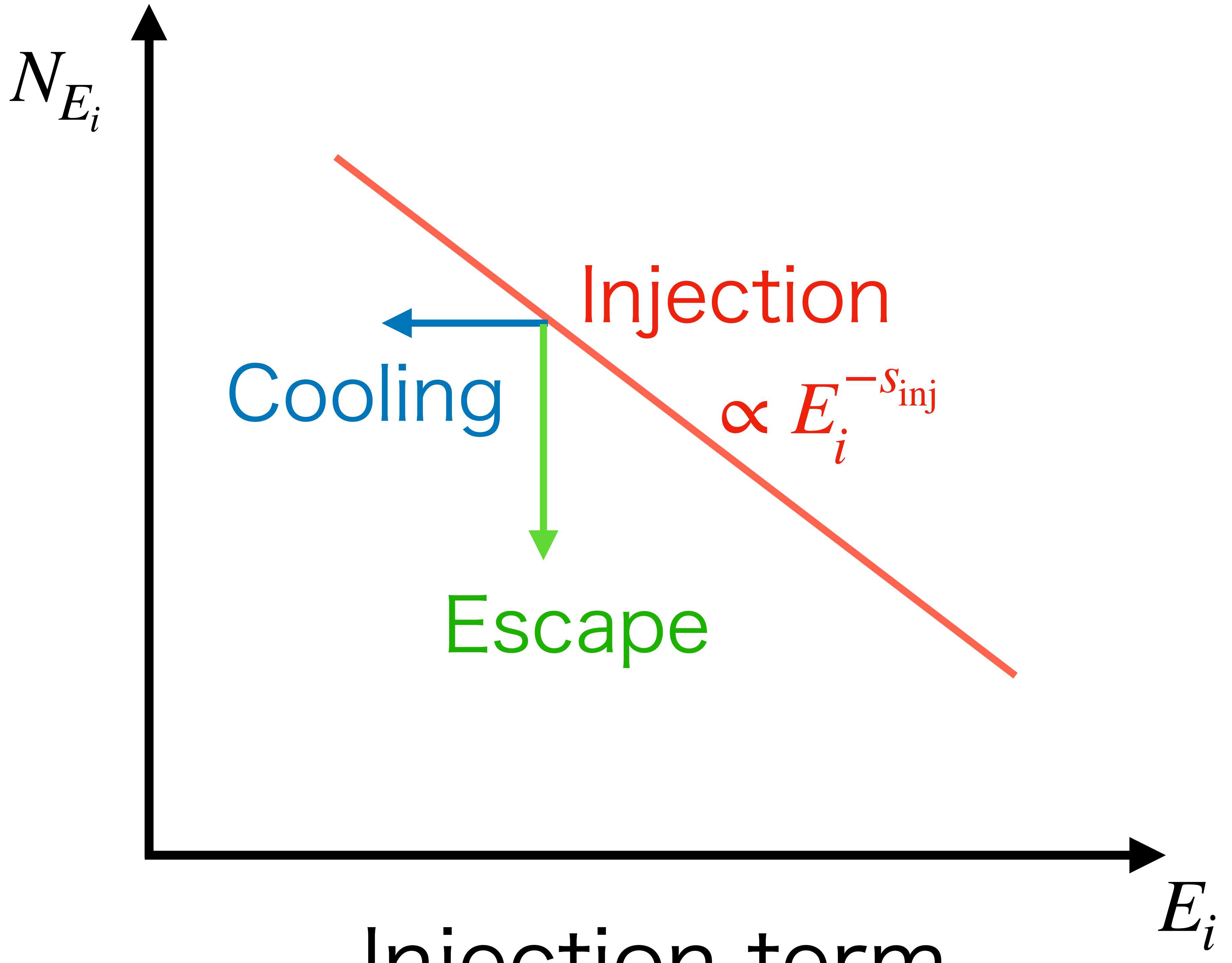

Injection term

$$\dot{N}_{E_{i.\mathrm{inj}}} = \dot{N}_0 \left(\frac{E_i}{E_{i,\mathrm{cut}}}\right)^{-s_{\mathrm{inj}}} \exp\left(-\frac{E_i}{E_{i,\mathrm{cut}}}\right)$$